Soils and Rocks
An International Journal of Geotechnical and Geoenvironmental Engineering
www.soilsandrocks.com
ISSN 1980-9743
ISSN-e 2675-5475

Toward sustainable tailings disposal: a geotechnical overview of Brazilian research

Márcio de Souza Soares de Almeida[1], Fernando Schnaid[2], Romário Stéffano Amaro da Silva[1#], Leonardo De Bona Becker[6], Bruno Guimarães Delgado[3,4,5], Antonio Jeronimo Pereira de Souza Junior[1], Frederico Wagner Alvarenga Oliveira[1], Maria do Carmo Reis Cavalcanti[6], Sparsha Sinduri Nagula[7]

Article

Keywords
Mine tailings
Tailings dams
Filtered tailings stacks
Liquefaction
Critical state soil mechanics

Abstract

Brazilian geotechnics plays a key role in the pursuit of safer and environmentally sustainable tailings disposal solutions. From that perspective, this paper outlines the Brazilian academia and industry contributions to the geotechnics of mining tailings, highlighting the main aspects of some recent studies carried out by Brazilian research groups. Firstly, a literature review focusing on Brazilian research, published mainly in the last decade, is first presented. Subsequently, aspects relating to the behavior of tailings dams are discussed, including statistical methods for accurately assessing strength parameters, static liquefaction susceptibility of tailings subjected to various stress paths, and numerical models used to evaluate the effect of triggers on the onset of liquefaction of upstream tailings dams. Finally, regarding filtered tailings stacks, increasingly viewed as a preferable option for tailings storage, topics related to particle breakage, transitional behavior, effects of undercompacted materials and static liquefaction susceptibility of iron and rare earth tailings are addressed.

1. Introduction

The role of the mining sector in the Brazilian economy increases the need for technically, socio-economically, and environmentally suitable alternatives for disposing of mining tailings. From this perspective, Brazilian geotechnics is a key player in the pursuit of engineering solutions capable of meeting the challenging demands generated by the large volumes of tailings being produced by the mining companies (Schnaid, 2019).

The simplicity of operation and lower initial costs have made tailings dams, or impoundments, the predominant type of tailings storage facility (TSF) globally. However, the vast quantities of loose and saturated sands and fines render these tailings susceptible to liquefaction. Consequently, tailing dams, particularly those raised using the upstream method, are inherently less stable than those constructed using alternative methods (e.g., Morgenstern, 2018).

Recent catastrophic failures of Fundão and Brumadinho have led to significant tightening of legal regulations by Brazilian authorities concerning the construction and management of conventional tailings dams. In response, filtered tailings stacks have emerged as a promising TSF alternative, primarily due to their potential to reduce the social and environmental impacts associated with dam failures. Filtration involves dewatering tailings using vacuum or pressure techniques to achieve a solids content exceeding 85% by mass. The resulting filter cake exits with controlled moisture content and is transported via conveyor or truck, placed, spread, and compacted to form a dense, stable, unsaturated tailings stack, here named filtered tailings stacks, preferred here to the incorrect term dry stack. This method eliminates the need for retention dams and tailings ponds (Watson et al., 2010; Davies, 2011; Delgado et al., 2023). In this context, research centers and industry have turned their attention to filtered tailings stacks (Carvalho et al., 2023).

[#]Corresponding author. E-mail address: romario.amaro@coc.ufrj.br
[1]Universidade Federal do Rio de Janeiro, Programa de Engenharia Civil/COPPE, Rio de Janeiro, RJ, Brazil.
[2]Universidade Federal do Rio Grande do Sul, Programa de Pós-Graduação em Engenharia Civil, Porto Alegre, RS, Brazil.
[3]Vale S.A., Belo Horizonte, MG, Brazil.
[4]Universidade do Porto, Construct-GEO Faculty of Engineering, Porto, Portugal
[5]Universidade Federal de Ouro Preto, Ouro Preto, MG, Brazil.
[6]Universidade Federal do Rio de Janeiro, Escola Politécnica, Rio de Janeiro, RJ, Brazil.
[7]Norwegian Geotechnical Institute, Oslo, Norway.

Submitted on December 28, 2024; Final Acceptance on June 5, 2025; Discussion open until November 30, 2025.
Editor: Renato P. Cunha
https://doi.org/10.28927/SR.2025.011624

The objective of the paper is to unite contributions from academia and the mining industry to highlight the present state of practice in Brazil regarding mining tailings. Initially the main studies developed by Brazilian authors in the last decades on this topic are highlighted. Subsequently, the behavior of conventional tailings dams is examined based on recent experimental data gathered from in situ and laboratory test campaigns, complemented by numerical analyses. Finally, recent studies on filtered tailings stacks are presented predominantly based on laboratory and field studies.

The background of modern mining tailings analysis, which is also considered in the present paper, is the critical state soil mechanics (CSSM), where the voids ratio (e) is recognized as a key parameter - together with stress state (mean effective stress, p', and deviator stress, q, which defines the mechanical behavior of soils (Schofield & Wroth, 1968). The CSSM has been well proven over the last half century to describe the in-situ behavior of soft clays (Almeida, 1982; Almeida & Ortigão, 1982). However, traditional CSSM does not adequately describe the behavior of mining tailings and granular geomaterials in general, particularly concerning dilatancy. The state parameter, ψ (Jefferies & Been, 2015) defined by the difference between the current/initial void ratio and the critical state void ratio (e_{cs}) for the same stress level is a key parameter to analyze mining tailings under both drained and undrained conditions (Been & Jefferies, 1985).

2. Brazilian contribution to mining tailings disposal

The final disposal of mining tailings, or even their reuse and recycling, has been a central theme in the major geotechnical research centers in Brazil. Schnaid et al. (2014) highlighted a background of research projects consisting of laboratory tests and field tests campaigns carried out in various parts of the country, at Tailings Storage Facilities (TSF) for iron, gold, bauxite, and zinc ores, at different stages of operation. Significant contributions to the practice include earth dams, downstream, upstream and centerline tailings dams, as well as filtered tailings stacks. Several aspects have been evaluated, including the geomechanical characterization of tailings, assessment of constitutive models, performance analysis and stabilization techniques. Despite the recent trend of designating these structures as TDF (Tailings Disposal Facilities), in this paper the designation TSF will be maintained as it is still more widely used among both researchers and practicing engineers.

Given the variability inherent in tailings from diverse origins and processes, significant efforts have focused on geotechnical characterization of samples from major beneficiation plants and TSFs in Brazil (Nery, 2013; André et al., 2018; Pölzl et al., 2018; Praca et al., 2019; Telles et al., 2019; Tinoco & Marinho, 2019; Becker et al., 2022; Quintelas et al., 2020; Bruschi et al., 2023; Quirino et al., 2022; Medina et al., 2023; Santos et al., 2023; Velten et al., 2024; Wagner et al., 2023; Consoli et al., 2024b; Dias Neto et al., 2024; Medina et al., 2024). Viana da Fonseca et al. (2022) reported the results of an extensive laboratory tests campaign on laboratory-compacted samples of iron ore tailings collected after the collapse of the B1 dam, providing physical, hydraulic, and mechanical characteristics of the tailings to support numerical backanalysis. Based on the premise that a greater similarity in terms of geotechnical characteristics and hydromechanical behavior is expected in tailings from the same geological formation, Carneiro et al. (2023) presented a database of iron ore tailings from the Brazilian Iron Quadrangle. The authors classified the materials into three categories, whose properties are summarized in Table 1.

The most common minerals found in these materials are iron, goethite, magnetite, and hematite. The compiled data represents an important indicator of the variability of the key material parameters, as well as ranges of values that can be adopted as a reference point. Figure 1 shows the particle size ranges of Iron Quadrangle tailings, with the pink zone representing plastic tailings. The white curve indicates the division between coarse and fine tailings within the blue zone.

Driven by the occurrence of numerous catastrophic accidents, a particular focus is given to the assessment of mine tailings' static liquefaction susceptibility. Bedin et al. (2012) studied the behavior of a gold ore tailing through conventional triaxial compression tests. Each specimen was compacted in three layers. The results were analyzed in the light of CSSM, and it was observed that the tendency towards total liquefaction was only identified in specimen subjected to low levels of confining stress. On the other hand, intermediate levels of confinement led to the occurrence of large deformations associated with high pore pressure generation, but without the complete loss of the material's shear strength (flow instability). A tendency for grain breakage was only noticed in tests with higher levels of confining stress. Schnaid et al. (2013) extended this study by identifying the state parameter (ψ) and the small strain shear modulus (G_0) as valid indicators of the static liquefaction susceptibility in the gold ore tailings studied. Pereira et al. (2006) analyzed

Table 1. Categories of Iron ore tailings from Brazilian Iron Quadrangle (from Carneiro et al., 2023).

Category	Grain size	Average mass density (g/cm^3)	Plasticity
Coarse tailings	Silty sand	3.63	Non-plastic
Fine tailings	Sandy silt	3.59	Non-plastic
Plastic tailings	Silt and clay	3.97	Average plasticity index of 13.4

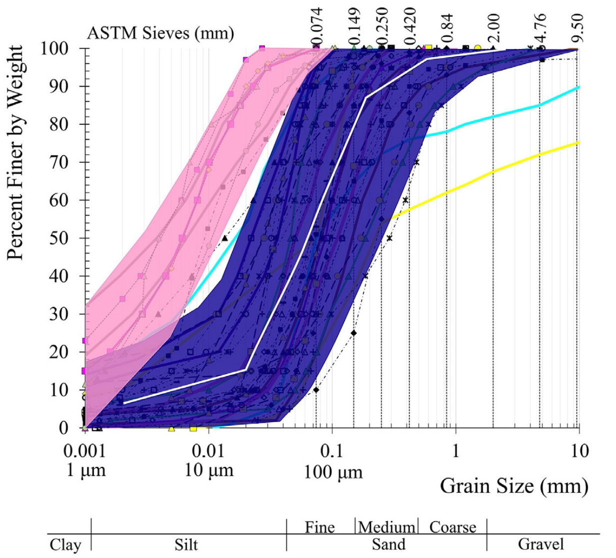

Figure 1. Particle size distribution zones of iron ore tailings from the Brazilian Iron Quadrangle, in which the pink zone covers plastic tailings, and the blue zone encompasses coarse and fine tailings, distinguished by the white curve (Carneiro et al., 2023).

the static liquefaction susceptibility of iron ore tailings from different plants in the Brazilian Iron Quadrangle. The authors verified that some tailings collapsed even at low strain levels, which indicates the importance of incorporating this aspect into TSF stability analyses. Besides the axial compression stress path, recent studies have highlighted the tendency for static liquefaction arising from non-conventional stress paths, such as lateral extrusion and *p'* reduction under constant deviatoric stress (CSD tests). Moreover, the sample preparation method may influence liquefaction behavior since it is difficult to reproduce in the laboratory the same particle arrangement found in hydraulically deposited tailings.

Several studies have addressed the interpretation of field tests, focusing on the susceptibility to liquefaction of tailings disposed in TSFs (Albuquerque Filho, 2004; Pirete & Gomes, 2013; Santos Junior et al., 2022). Quirino et al. (2022) and Viana da Fonseca et al. (2022) found that the proportion of non-plastic fines has little influence on the effective friction angle of a sandy iron ore tailings but highly influences the position of the CSL in the compressibility plot, $e - \ln p'$.

Espósito et al. (2002) developed a methodology for quality control during the construction of upstream tailings dams, with a probabilistic and observational approach, which considers the void ratio variability along the structure built as a hydraulic embankment and allows the evaluation of its liquefaction potential. Cavalcante et al. (2012) created a numerical method that represents the deposition mechanism of hydraulically transported tailings. Studies on the effects of earthquakes on the stability of tailings dam have also been conducted, focusing on the particularities inherent to Brazilian seismicity (e.g. Agurto-Detzel et al., 2016; Ayala et al., 2020), where seismic accelerations range from 2.5% to 15% of gravity due to its position in the middle of a tectonic plate. However, Brazil is still in an early stage of developing studies that consider the effects of seismic loading under TSF.

Regarding the analysis of the TSF's stability, particularly with respect to the consequences of static liquefaction, the application of NM has become a prevalent approach. NM have the benefit of making it possible to simulate the behavior of the structure during its raisings and according to the occurrence of various liquefaction triggers. In this sense, NM has been routinely used in tailings dam failure back analyses (Morgenstern et al., 2016; Arroyo & Gens, 2021). Limit-equilibrium analyses were successfully applied to a real case, through the accurate definition of the stratigraphy, strength of the reservoir's component materials, pore pressures and shapes of the failure surfaces (Becker et al., 2023b). It is important to note that limit equilibrium methods estimate the ultimate stress state preceding failure without accounting for the effects of progressive failure on the structure and its foundation. Consequently, caution is warranted when applying these methods to materials prone to strain-softening prior to failure.

Given the importance of using constitutive models in NM that adequately represent the behavior of the materials, Faria et al. (2023) compared experimental data from a laboratory testing campaign of an iron ore tailings from the Iron Quadrangle with results obtained from the calibration of the Modified Cam-Clay and NorSand constitutive models, both based on CSSM. The NorSand model accurately predicted stress-strain behavior and the stress paths of isotropically consolidated drained (CID) triaxial compression tests. A similar comparison was carried out by Coutinho et al. (2025) for isotropically consolidated undrained (CIU) triaxial compression tests, also for iron ore tailings, showing a good agreement between these tests and the Norsand model (Figure 2).

Costa et al. (2024) also demonstrated the successful application of the NorSand model to simulate the strain-softening behavior of the material. However, they noted the high sensitivity of the numerical simulation responses to the parameters of the constitutive model, highlighting the importance of accurate and reliable experimental data for calibration.

Rógenes et al. (2025) re-simulated the B1 Dam Failure in Brumadinho using a numerical hydromechanical flow coupling code with two constitutive models, CASM (Arroyo & Gens, 2021) and NorSand. The authors were able to conclude that the most important aspect related to the constitutive model in assessing structures susceptible to static liquefaction lies in the constitutive model's capacity to represent the sudden strength loss due to pore pressure generation. Even though the NorSand model assumes an associated flow rule, the model was able to simulate the failure conditioned by two hypothetical triggers: dam loading and gravity increase. However, NorSand simulations required slightly more

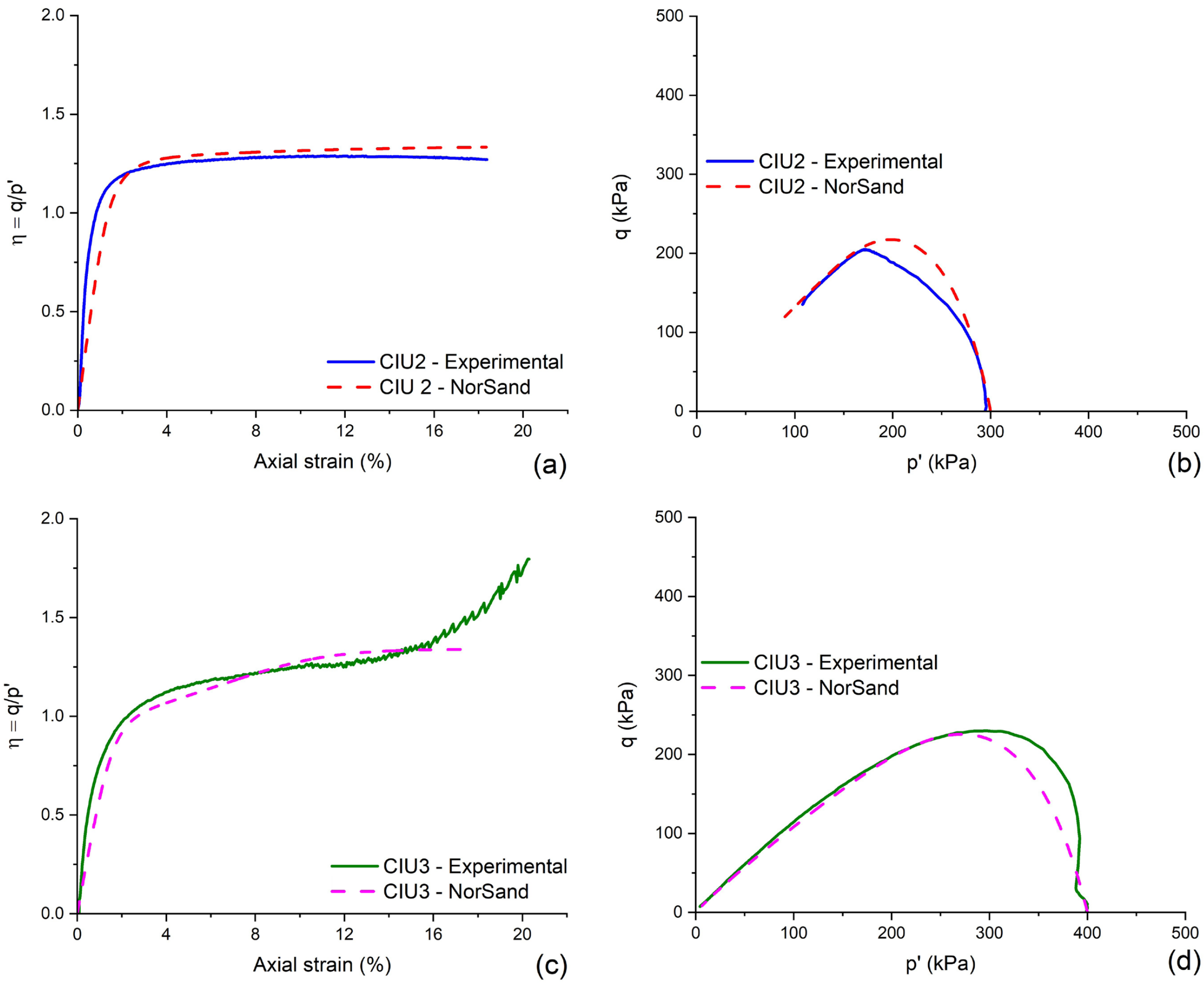

Figure 2. Comparison between laboratory test results and simulation using a calibrated NorSand model (Coutinho et al., 2025).

pronounced disturbances to activate the failure mechanism (twice the value of dam load and 1.4 times higher gravity increase than those required to trigger the failure with the CASM simulations).

Carvalho et al. (2024) have demonstrated that some iron ore tailings do not follow an associated flow rule, which is an assumption adopted by currently used CSSM constitutive models. These aspects underscore the need for constitutive models specifically developed to better represent tailings behavior (non-textbook geomaterials), considering fabric, mineralogy, particle morphology, non-associated plastic flow rules and stress-history. In addition, considering the current tendency towards high height filtered tailings stacks, there is a demand for constitutive models that can accurately simulate tailings behavior in unsaturated conditions and with the incorporation of some particle size distribution and morphology.

Due to the characteristics of TSFs, the development of alternative disposal solutions has become an important focus of research. Geosynthetics have been used in tailings dam drainage systems (Araújo et al., 2010) and in tailings dewatering systems (Bittar et al., 2010). Silva et al. (2021) were able to validate analytical and numerical methods for predicting the behavior of geotubes used to dewater gold ore tailings. Palmeira et al. (2010) studied the performance of non-woven geotextiles applied as drains and filters in tailings dams and observed that conditions encountered in certain regions of the structure, such as in the vertical drainage system, indicate the need for further studies and laboratory tests to better replicate field conditions, as well as careful assessment of the occurrence of severe clogging and the geotextile durability.

3. Tailings dams

3.1 Introduction

Some recent tailings dam failures (Mount Polley, Cadia, Fundão & B1 in Brumadinho) highlighted the need for a better understanding of the tailing's geotechnical behavior for safer TSF. In Brazil, the construction and operation of upstream tailings dams has been prohibited, thus imposing the closure of these structures (Brasil, 2019). Local country guidelines (e.g., ANCOLD, 2019; CDA, 2013, 2019) along with international guidelines (e.g., ICOLD, 2005; ICMM, 2020) govern TSF design and performance worldwide.

In Brazil, the main guideline to be followed for the design of Tailings Storage Facilities is the NBR 13028 (ABNT, 2013), although international guidelines are also adopted. However, Brazilian legislation (e.g., Brasil, 2019; ANM, 2022) is the main driving factors for mining tailings design and performance in Brazil.

3.2 Peak and critical state friction angles for non-plastic tailings

Traditionally, tailings strength has been evaluated using deterministic methods. However, given the inherent heterogeneity of tailings, a statistical approach is more suitable for accurately representing their behavior. The current body of literature on the distribution of tailings strength is both sparse and superficial, which hinders the probabilistic analyses critical for effective risk management.

Becker et al. (2023a) investigated the probability density functions of the peak friction angle and relative density of sand tailings from the Germano dam reservoir in Mariana, Brazil. Utilizing publicly available CPTu data, their study also highlighted the significant influence of disperse plastic layers on the strength of sand tailings.

The sand tailings from the Germano reservoir consist primarily of silty sand, incorporating quartz, iron oxides, hematite, and goethite. The fines consist entirely of silt. The iron ore mining and tailings disposal processes, marked by frequent changes in discharge points lead to the development of a heterogeneous stratigraphy, characterized by randomly distributed layers of plastic tailings scattered between the sand tailings. Interpretation of CPTu data in this type of stratigraphy is complex, since the cone tip resistance is influenced by the material properties both ahead and behind the penetrating cone (Treadwell, 1976). The zone of influence around the cone in soft materials can be as small as two to three cone diameters, whereas in stiffer materials, it can extend up to 10 to 20 cone diameters (Lunne et al., 1997). The area of influence in sand layers also depends on their relative density and horizontal stress state (Ahmadi et al., 2005).

To more accurately assess the heterogeneity of coarse tailings in the characterization of the Germano reservoir, four distinct scenarios were evaluated:

- Scenario 1: Analysis of all measurements classified as sand tailings (I_c < 2.6, corresponding to types 5 and 6 in the Robertson (2016) soil classification chart), without excluding any data;
- Scenario 2: Outlier removal – measurements with peak friction angle ($\phi_p^{'}$) values exceeding mean value plus three times the standard deviation or falling below mean value minus three times the standard deviation were discarded, resulting in the exclusion of approximately 0.3% of the data;
- Scenario 3: Exclusion of measurements potentially influenced by adjacent layers of plastic tailings – data within the first 0.20 m and the last 0.35 m of any sand tailings layer were discarded, following Ahmadi et al. (2005) criteria, conservatively assuming a relative density of 50%;
- Scenario 4: A combination of scenarios 2 and 3 – outliers were removed after discarding measurements potentially influenced by the plastic tailings layers.

Two correlations were employed to estimate the peak friction angle ($\phi_p^{'}$) from CPTu tests in this research. The first, Equation 1, was developed by Kulhawy & Mayne (1990) for uncemented, clean, rounded sands, based on flexible-walled CPT calibration chamber test data, in which Q_{tn} is the normalized cone resistance. The second, Equation 2, proposed by Robertson & Campanella (1983), estimates the peak friction angle using spherical cavity expansion theory and plasticity limit formulation, in which q_t is the cone resistance and σ'_{vo} is the effective vertical normal stress.

$$\phi_p^{'} = 17.6 + 11 \log Q_{tn} \tag{1}$$

$$\phi_p^{'} = \tan^{-1}\left[0.1 + 0.38\log\left(\frac{q_t}{\sigma'_{vo}}\right)\right] \tag{2}$$

When both correlations are applied, for all four scenarios, the mean peak friction angle ranged between 33° and 35°, consistent with the peak friction angles reported for iron ore tailings dams in the same region of Brazil (Pereira, 2005; Consoli et al., 2023; Farenzena, 2024). The standard deviation varied between 1.9° and 2.5°. The probability density functions of the peak friction angle for sand tailings from the Germano Dam's main reservoir, as estimated through correlations with CPTu tests, closely followed a normal distribution.

The discard of cone tip resistance measurements near the boundaries of the sand layers, when there are interspersed, plastic tailings layers, reduces the influence of these plastic layers in the assessment of the sand tailings parameters. From the data analyzed by Becker et al. (2023a), this discarding process resulted in an approximate 1° increase in the mean friction angle, while the standard deviation remained unchanged. This finding underscores the importance of this exclusion step when assessing friction angles using CPTu data. Conversely, the removal of outliers had little to no impact on the results.

Coutinho (2022) related both peak friction angle ($\phi_p^{'}$) and critical state friction angle ($\phi_{cs}^{'}$), with the initial state parameter ψ_0 obtained from a campaign of triaxial tests carried out on non-plastic tailings. Figure 3 shows the data basis plots of $\phi_p^{'}$ versus ψ_0 developed by Jefferies & Been (2015) together with seven drained triaxial tests performed by Coutinho (2022). The peak friction angle $\phi_p^{'}$ decreases with the increase of the absolute values of the state parameter ψ_0, with Coutinho (2022)'s data fitting well into the database.

It is also interesting to analyze the graph of the difference ($\phi_p^{'}$ - $\phi_{cs}^{'}$) versus ψ_0, as shown in Figure 4. It is clearly observed that ($\phi_p^{'}$ - $\phi_{cs}^{'}$) decreases with the increase of the absolute values of ψ_0. Or, in other words, as the soil transitions from dilating to contracting, the peak friction angle $\phi_p^{'}$ gets closer to the critical state friction angle $\phi_{cs}^{'}$.

Jefferies & Been (2015) proposed an equation relating $\phi_p^{'}$ and ψ_0 (Equation 3), based on an average critical state friction angle of 32° for quartz sands. The authors argue that this equation is broadly applicable, regardless of grain size and shape, fines content, or mineralogy. This equation is plotted as a dashed green line in Figure 3 and shows a good fit for the triaxial tests performed by Coutinho (2022).

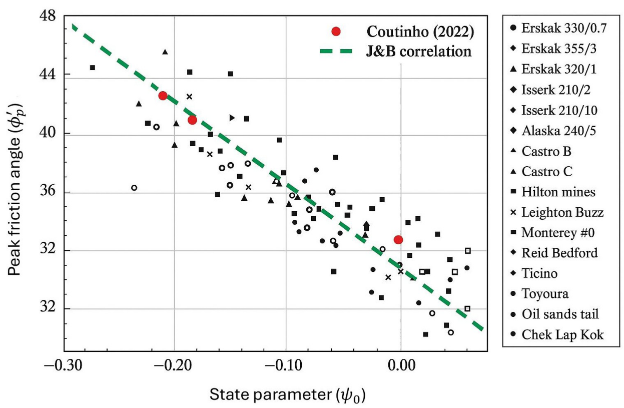

Figure 3. Peak friction angle versus initial state parameter (Jefferies & Been, 2015, modified by Coutinho, 2022).

$$\phi_p^{'} = \phi_{cs}^{'}\left(1-\frac{5}{3}\psi_0\right) \tag{3}$$

3.3 The brittleness index for non-plastic tailings

The brittleness index (I_{BU}) (Bishop, 1969, 1973) relates the peak undrained strength ($s_{u,peak}$) to critical state undrained strength ($s_{u,liq}$) (Equation 4). I_{BU} is a useful parameter to assess the potential for post-peak loss of undrained shear strength of a material in an undrained condition. An I_{BU} value equal to 1 indicates a material prone to complete liquefaction, since the $s_{u,liq}$ value tends to 0.

$$I_{BU} = \frac{s_{u,peak} - s_{u,liq}}{s_{u,peak}} \tag{4}$$

Coutinho (2022) evaluated the influence of the initial state parameter on I_{BU} values for the tailings in his study, as well as for those from the Germano Dam, reported by Telles (2017) (Figure 5). For these tailings from the Brazilian Iron Quadrangle, a linear correlation can be observed between the initial state parameter and the I_{BU}. An increase in ψ_0 leads to a higher I_{BU}, due to an increase in the $s_{u,peak}$ and a decrease in $s_{u,liq}$.

Saar et al. (2024) highlighted the need for a case-by-case interpretation of iron ore tailings, given that their behavior is strongly influenced by mineralogy, morphology, and fabric. In the sandy-silty tailings studied, partial drainage was detected during CPTu tests, which underscores the need for adjustments in the piezocone penetration rate when used in non-textbook materials (Schnaid et al., 2021). Using an inappropriate rate in some in-situ tests, such as the Vane Test, makes data interpretation particularly complicated. In these cases, the design parameters must be defined in consonance

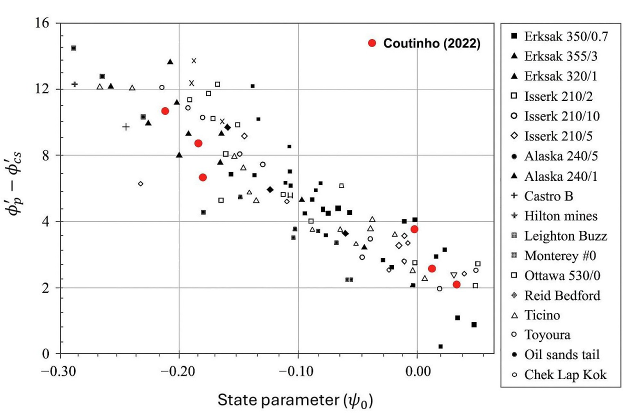

Figure 4. $\phi_p^{'}$ - $\phi_{cs}^{'}$ versus initial state parameter (Jefferies & Been, 2015, modified by Coutinho, 2022).

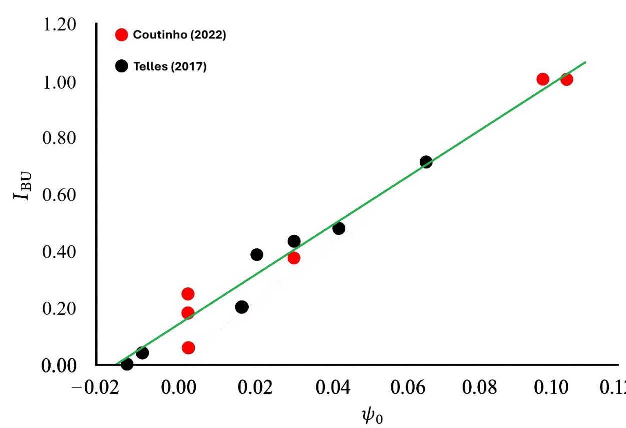

Figure 5. Linear correlation between initial state parameter and brittleness index for iron quadrangle tailings (Coutinho, 2022).

with laboratory tests data. In addition, it is important to note that the case-by-case interpretation premise is valid for tailings from other ore types, given that each type has its own particular properties.

3.4 Undrained strength parameters for plastic tailings

Becker et al. (2024) analyzed the characteristics, and the strength of iron ore plastic tailings found in a dam in Minas Gerais state, Brazil. This material is like other plastic tailings originating from iron ore in the same state and is composed of a reddish mixture of silt-sized and clay-sized particles. Clay-minerals are almost absent, and the presence of iron oxides results in a specific gravity of particles (G_s) between 3.9 and 4.0. The plasticity index is low, ranging between 7% and 11%. These tailings have a coefficient of consolidation within the same range of normally consolidated clays of similar plasticity and their permeability is also low (k < 10^{-8} m/s). After identifying and selecting only plastic tailings and discarding results of other materials, 845 layers of plastic tailings were found in 31 CPTu tests. These layers presented low tip resistance, friction ratio below 2%, and high values of positive excess pore pressure. The Soil Behavior Classification Index (Robertson, 2009, 2016), I_c, exceeds 2.95, and these materials are classified as "silty clay to clay". It should be noted that the same layer often appears in several tests, and the plastic tailings are sometimes found amid layers of sand tailings. Sixty-seven field vane tests performed near the CPTu tests allowed the estimation of the cone factor (N_{kt}). A log-normal distribution was found with a mode of 16.2, and median of 19.4. The normalized peak undrained strength ratio ($s_{u,peak} / \sigma'_{v,0}$) based on the N_{kt} median showed a lognormal distribution with mode of 0.159, and median of 0.207 (Figure 6). These values are significantly lower than the peak undrained strength of the sand tailings originated from the same iron ore, as well as other sand tailings indicated in the literature.

A particular concern today in Brazil is the definition of geotechnical parameters for geomechanical modeling of upstream tailings dams undergoing de-characterization. In this regard, data from in-situ and laboratory test campaigns were jointly analyzed to provide an accurate interpretation of the expected tailings behavior.

3.5 Static liquefaction trigged for lateral extrusion

Recent investigations into the TSF failures at Fundão and Cadia have identified a significant factor contributing to liquefaction: strain softening and associated deformations of the underlying fine-grained soils. These deformations lead to an increase in deviator stress (q), a decrease in mean effective stress (p'), resulting in an increased stress ratio (η) in the overlying loose, saturated tailings. This mechanism was initially termed "basal extrusion" by Jefferies & Been (2015) and was subsequently renamed "lateral extrusion" (LE) by Morgenstern et al. (2016).

Given that the primary condition to achieve an LE stress path is maintaining constant vertical stress, it can be mathematically demonstrated that under axisymmetric conditions (i.e., triaxial conditions), this stress path has a slope of -1.5 in the deviator versus mean effective stress space. Another crucial feature of the LE stress path is its similarity to the constant shear drained (CSD) path. In this path, conditions are presumed to remain largely drained until the stress ratio (η) exceeds the instability stress ratio (η_{IL}) for a specific soil state. An illustration of the LE stress path is provided in Figure 7.

However, as suggested by Jefferies et al. (2019), due to the significant volumetric strain observed in loose materials, this stress path may occasionally involve small increments of deviator stress under undrained conditions. This drained-

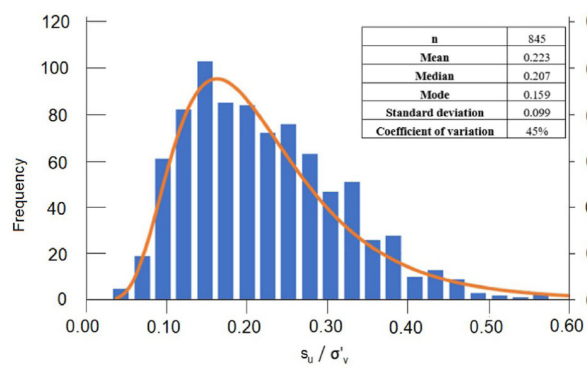

Figure 6. Histogram and lognormal distribution for all layers of plastic tailings based on the N_{kt} median, discarding CPTu measurements taken at distances of less than 0.05 m from the sand layers (Becker et al., 2024).

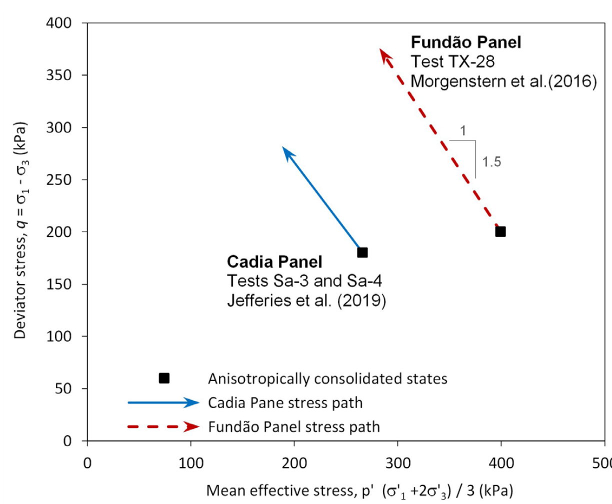

Figure 7. Schematic illustration of the lateral extrusion stress path inferred by the Fundão and Cadia panels (Souza et al., 2024).

to-undrained transition may occur in field conditions due to extended drainage paths or minor disturbances that generate excess pore pressure beyond the material's dissipation capacity.

The triggering of instability under the lateral extrusion stress path was extensively studied by Souza et al. (2024) on silica fine sand (SFS). A series of 12 LE triaxial tests were conducted, employing three distinct testing procedures to investigate the instability behaviour under varied drainage and stress path conditions. The first consisted of conventional undrained compression (CAU) tests. In the second procedure, the stress path was followed in a drained manner, meaning the drainage valves were open, allowing the specimen to drain during the entire extrusion process. The third procedure sought to replicate the undrained increments described by Jefferies et al. (2019). In this approach, the LE stress path was followed while incorporating several small, undrained increments of 5 kPa, 10 kPa, or 20 kPa of deviatoric stress, each applied over three minutes. These increments were followed by drained stages of equal duration, lasting three minutes. The study by Souza et al. (2024) investigated sand instability under three primary loading conditions: undrained compression (CAU), fully drained lateral extrusion, and lateral extrusion with alternating drained and undrained stages. Rather than targeting a single state condition, the test program for each loading scenario was designed to encompass a range of initial state parameters, which varied from -0.02 to +0.09.

The determination of the onset of instability in LE and CSD tests typically involves the assessment of the strain rate versus time graph ($\delta \varepsilon_a$ versus δt). For LE tests, where a constant vertical stress must be maintained throughout the extrusion, the onset of instability, as determined by the assessment of the $\delta \varepsilon_a$ versus δt plot, coincides with the point where the equipment can no longer maintain a constant vertical stress condition (Souza et al., 2024). An illustration of the onset of instability during a triaxial LE test is shown in Figure 8, which presents plots of vertical stress and axial strain ratio over time. A noticeable change in the trend can be observed in both graphs. In this case, the rapid increase in axial strain ratio and the corresponding decrease in vertical stress are attributed to the liquefaction of the specimen.

The results obtained by Souza et al. (2024) demonstrated that during the drained LE stress path, the SFS can achieve high values of axial strain rate at instability (between 5 and 28%/min) with negligible excess pore pressure (below 2 kPa). This supports the statements of many other authors (Eckersley, 1990; Sasitharan et al., 1993; Skopek et al., 1994) that excess pore pressure observed after flow liquefaction is a consequence of the collapse and not its cause. However, the tests with undrained increments demonstrated that even short undrained stages during the LE stress path can significantly reduce η_{IL}, leading to flow liquefaction occurring much earlier than would be predicted based on drained LE tests. Figure 9a illustrates the stress paths followed during five instability tests conducted by Souza et al. (2024) and the corresponding development of excess pore pressure throughout the LE tests. It can be observed that the alternating transitions between undrained and drained stages cause the stress path to shift leftward due to the positive excess pore pressure generated during the undrained stage. Subsequently, the stress paths (Figure 9a) shift back to the right, aligning with the original inclination of the LE stress path, during the drained stage. Additionally, Figure 9 shows that LE tests conducted with the drainage valves open throughout the entire extrusion process exhibit higher instability stress ratios compared to tests with undrained increments and the CAU test.

Souza et al. (2024) also interpreted the results of the instability tests using the modified state parameter approach

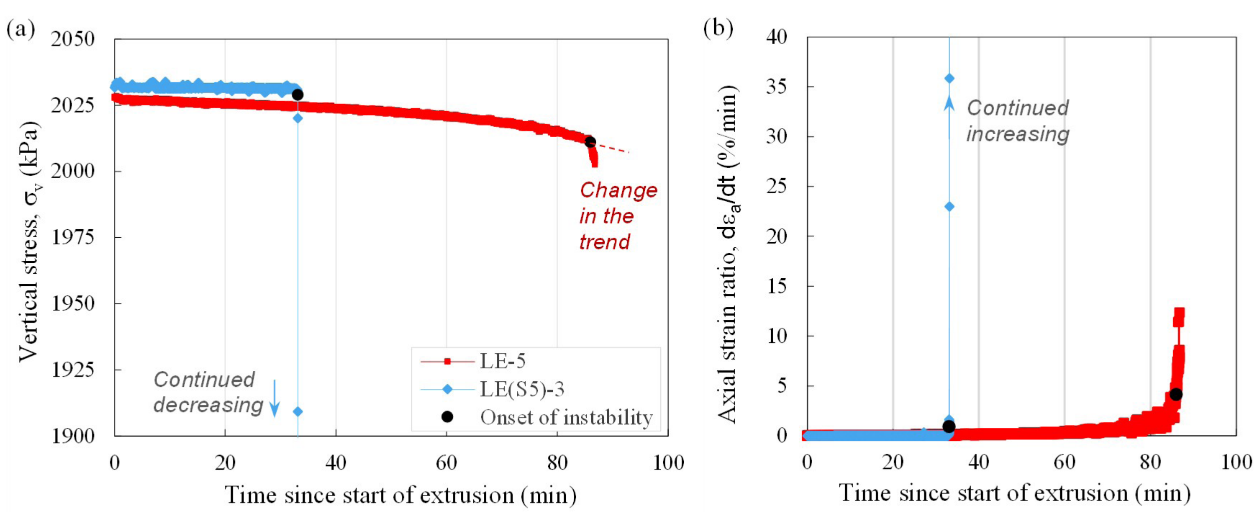

Figure 8. Interpretation of the onset of instability adopted in LE tests from Souza et al. (2024): (a) Changes in vertical stress over time; (b) Correspondent changes in axial strain rate. (reproduced from Souza et al., 2024).

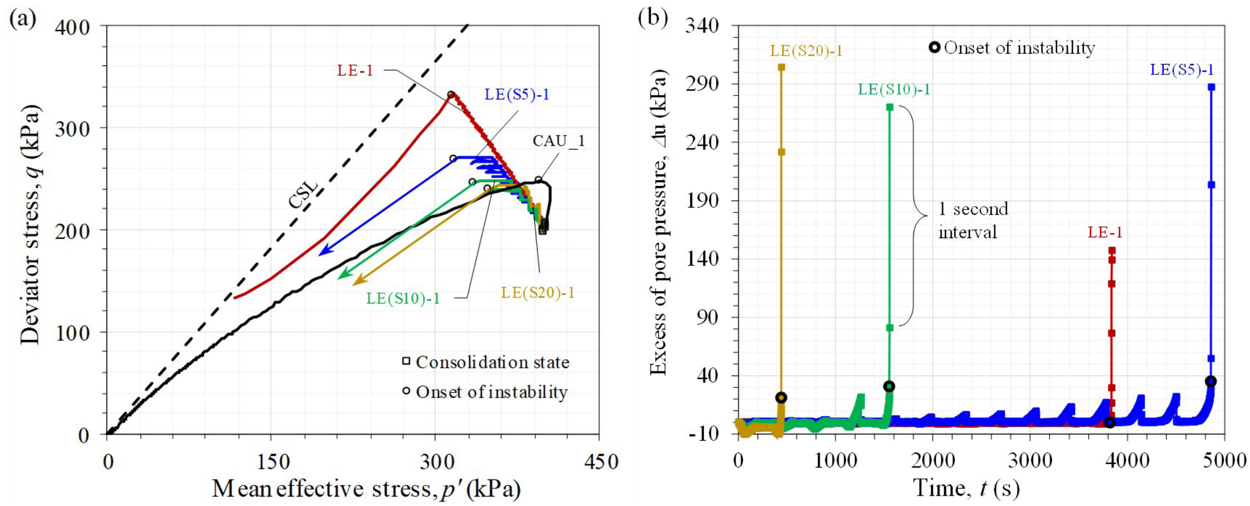

Figure 9. Instability tests with ψ_0 = 0.050 ± 0.003 (a) Effective stress paths; (b) Development of excess pore pressure over time. (reproduced from Souza et al., 2024).

(Chu et al., 2003). The modified state parameter values ranged from -0.03 to +0.08. For similar modified state parameter values, the drained lateral extrusion stress path resulted in the highest value of η_{IL}, followed by the CSD tests, then the lateral extrusion with undrained/drained stages (where smaller stress increments, δq, led to higher η_{IL} values), and lastly, the CAU triaxial test.

3.6 Hollow cylinder lateral extrusion tests

Souza (2023) expanded upon the findings of Souza et al. (2024) by investigating the LE mechanism using the Hollow Cylinder apparatus. This equipment overcomes some of the limitations of triaxial tests by enabling the rotation of principal stresses and allowing for independent control of the intermediate principal stress (σ_2). By varying the parameters of the principal stress angle (α) and the intermediate stress ratio (b), the tests can more accurately replicate in situ conditions, such as those observed below slopes, where the major principal stress is no longer aligned with the vertical axis (Reid et al., 2022a).

Studies have shown that soils generally exhibit reduced strength at small to medium strains as α increases (Uthayakumar & Vaid, 1998; Shibuya et al., 2003; Reid et al., 2022b), a phenomenon known as cross-anisotropy. This below-slope condition was simulated in the study by Souza (2023) through a series of hollow cylinder tests conducted on Silica Fine Sand (SFS) and Fundão Sand Tailings (FST), employing a range of α and b values.

The rotation of the principal stresses and the control of the intermediate stress in a hollow cylinder test are achieved by independently adjusting the pressure applied to the specimen's inner bore and outer surface, as well as the torque applied to its base. Figure 10 illustrates a hollow cylinder specimen alongside a schematic representation of the corresponding stress conditions.

Souza (2023) conducted 28 instability tests, comprising 9 triaxial (TX) and 19 hollow cylinder (HC) tests, with 18 tests performed on FST and 10 on SFS. The Critical State Line (CSL) for the FST material was established using CID and CIU tests on loose specimens. For FST, values of α ranged between 0 and 45°, with b values set at either 0 or 0.25. Conversely, α values in the SFS tests were either 0 or 22.5°, while b was also set at either 0 or 0.25.

Souza (2023) demonstrated through hollow cylinder LE tests on both SFS and FST materials under varying α and b values that lower instability stress ratios were obtained when α and b were non-zero. Furthermore, as α and b increased, η_{IL} decreased, a trend also observed by Fanni et al. (2024) in CSD tests.

Additionally, the results from Souza (2023) revealed that volumetric strain behaviour varied based on the type of loading applied during the extrusion stage. For both TX and HC tests conducted under identical consolidation conditions, the drained extrusion tests exhibited faster contraction than those with undrained increments. This suggests that following the LE stress path with undrained increments would result in a looser state at the same mean effective stress, compared to following the same path in a drained manner.

The findings presented by Souza (2023) highlight the significance of the lateral extrusion stress path in understanding soil instability and liquefaction mechanisms, particularly in loose, saturated tailings. Drained LE tests demonstrated high instability stress ratios, while undrained increments significantly lowered η_{IL}, confirming the sensitivity of liquefaction onset to drainage conditions. Moreover, the hollow cylinder tests revealed that cross-anisotropy, represented by variations in α and b, substantially influences instability stress ratios,

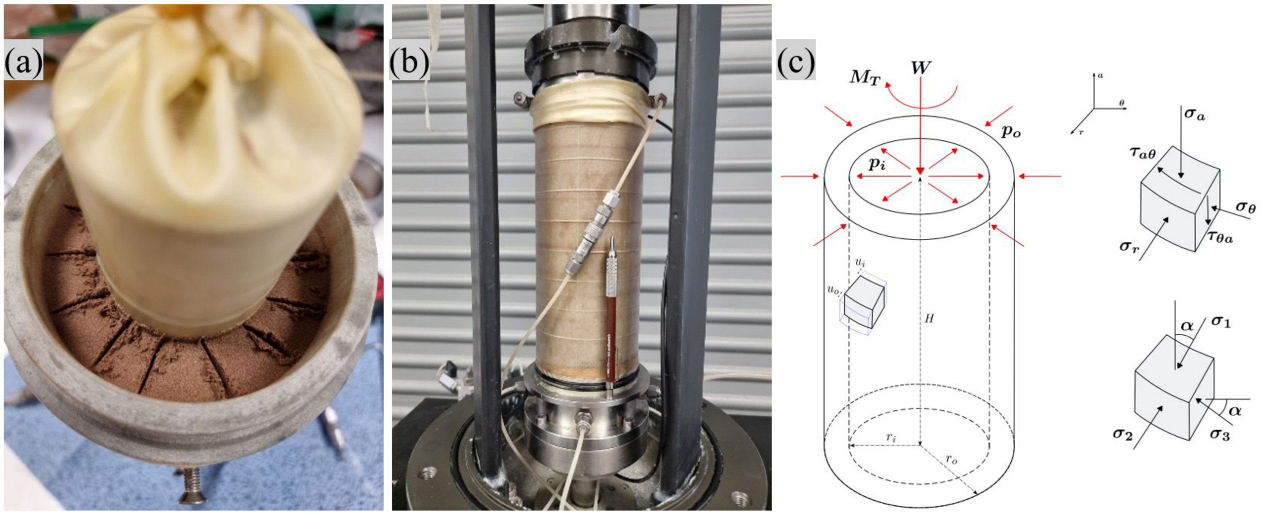

Figure 10. Hollow cylinder specimen: (a) specimen during moist tamping; (b) previous to cell closure; (c) stress conditions within the specimen (reproduced from Fanni et al., 2022a).

offering valuable insights into in situ stress states. These results underscore the need to account for realistic stress paths and anisotropic conditions in geotechnical design and failure analysis.

3.7 Assessing static liquefaction susceptibility for a tailings dam through a hydromechanical coupled numerical model

Numerical modeling has been an essential tool for assessing stability and particularly the static liquefaction susceptibility of Tailings Storage Facilities (TSFs), in which numerous boundary conditions and scenarios capable of leading to failure can be investigated. However, this can only be done if the materials composing the structure are represented by constitutive models that can simulate its real mechanical behavior, and more specifically simulate the liquefaction phenomenon.

There are several historical cases of TSF failure analysis using numerical models (NM) reported in the literature (e.g., Zabolotnii, 2020; Jefferies et al., 2019; Morgenstern et al., 2016; Robertson et al., 2019; Arroyo & Gens, 2021). Ledesma et al. (2022) states that the primary liquefaction triggers considered in this type of analysis are the rise in the phreatic surface within the tailings, horizontal displacements at the toe of the downstream slope and a surface load applied on the crest of the TSF. However, there is a lack of studies on the analysis of the conditions of TSFs in service, especially regarding analysis of unconventional critical scenarios.

Coutinho et al. (2025) performed stability analyses of a 77 m high Brazilian Iron Quadrangle tailings dam, using a hydromechanical coupled Finite Element numerical model. The study focused on assessing the tailings dam susceptibility to static liquefaction, considering a scenario of clogging of the internal drainage system (reducing its initial permeability coefficient by a factor of 1000) associated with the elevation of the phreatic surface in the impoundment. This critical situation, although hypothetical, may occur in a deactivated TSF because of inadequate maintenance, combined with heavy rainfall. This series of conditions can arise in many mining regions around the world.

The tailings dam uses a cyclone tailings disposal process that separates the iron ore tailings into two types: underflow and overflow tailings. The underflow material is deposited and compacted downstream, while the overflow is stored in the impoundment.

The triaxial tests used well recognized techniques (Viana da Fonseca et al., 2021; Jefferies & Been, 2015; Reid & Fanni, 2020) such as moist tamping and free ends, as well as void ratio at the end of the test determined by the freezing technique. Drained and undrained triaxial using predominantly loose specimens allowed the determination of critical state lines in the $q:p'$ and $e:\ln p'$ plots, as shown in Figure 11, with respective equations $q = M_{tc} p'$ and $e = \Gamma - \lambda \ln p'$ shown inside Figure 11.

The parameter M_{tc} (critical state friction ratio obtained from triaxial compression) is equal to 1.19, Γ (void ratio at reference pressure of 1 kPa) is equal to 0.932, and λ (slope of the CSL) is equal to 0.023. Jefferies & Been (2015) recommend that the parameter M used in the Norsand model is obtained from the triaxial tests from dense specimens. Figure 12 shows a plot of the peak stress ratio (η_{max}) against the minimum dilatancy (D_{min}), the ratio between volumetric and shear strains. As shown in Figure 12, the plot yielded values of $M = 1.34$ and $N = 0.31$, the latter named Volumetric coupling in stress dilatancy.

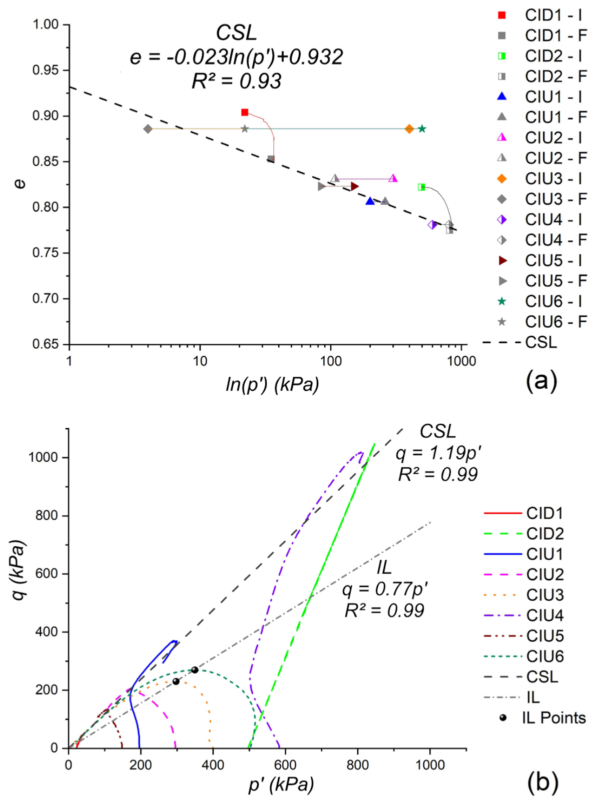

Figure 11. Critical state line in (a) $q : p'$ and (b) $e : \ln p'$ plots (Coutinho et al., 2025).

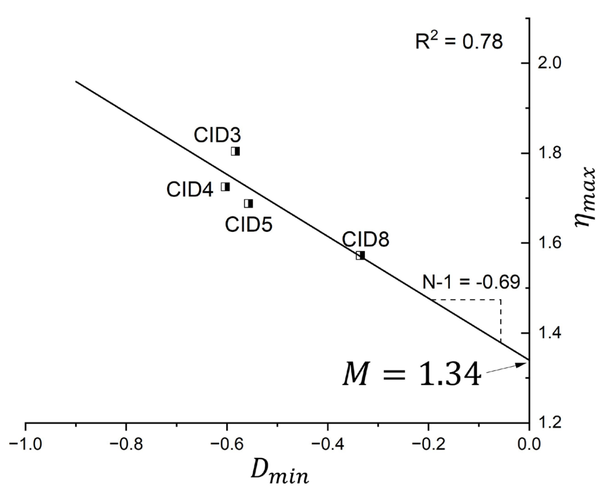

Figure 12. Peak stress ratio (η_{max}) as a function of minimum dilatancy (D_{min}) (Coutinho et al., 2025).

Figure 13 presents the cross-section of the dam, comprising a twenty-six-meter-high starter dyke built with compacted soil, and the downstream slope raised with compacted underflow tailings. The overflow material was stored in the impoundment. Unlike the conventional upstream construction model, in this structure, the lifts consist of compacted downstream underflow tailings above the starter dyke, which serves as the foundation for these lifts and helps to increase the stability of the dam. The structure has an average slope of 1V:2H, with downstream berms five meters wide every ten meters in height, resulting in a flatter slope of 1V:3.4H.

The underflow and overflow tailings, despite the segregation process, presented similar grain sizes distributions. For this reason, only the underflow material was the subject of an experimental campaign. The tailings are non-plastic fine silty sand, composed of 52% sand, 46% silt and 2% clay, with D_{50} = 0.06 mm, compatible with the range of values reported by Carneiro et al. (2023) for mining tailings from the Iron Quadrangle. These materials were modeled using the NorSand constitutive model (Jefferies, 1993; Jefferies & Been, 2015), based on the Critical State Soil Mechanics framework. NorSand has been successfully used to simulate the behavior of sandy and silty materials, especially at typical stress levels observed in most TSFs (Costa et al., 2024; Faria et al., 2024; Ghafghazi & Shuttle, 2008). Numerical simulations have demonstrated the efficacy of the NorSand model in addressing real-world scenarios encountered in TSF analysis (Brien et al., 2021; Shuttle et al., 2021).

To assess the Critical State Line (CSL) and the Instability Line (IL) of the underflow tailings, a series of 12 isotropically consolidated drained (CID) and undrained (CIU) triaxial tests were performed. However, for more realistic investigations, the authors understand that a broader discussion on the K_0 values used in such simulations would be important, since hydraulically disposed tailings typically present K_0 values lower than 1 (Rógenes et al., 2025). To circumvent this, it is ideal to also model the construction phases of the dam as documented in construction reports.

In addition, these triaxial tests plus eight bender elements tests and five resonant column tests were used to calibrate NorSand parameters. The initial void ratio of the undeflow material was set to represent the state parameter value closer to zero, which reflects the actual condition of the TSF based on the results of a CPTu test campaign.

Table 2 summarizes the NorSand parameters calibrated for the tailings. Additionally, the slope of the instability line (η_{IL}) is given by a stress ratio of 0.77. The calibrated NorSand model was able to accurately replicate the experimental results of the CIU and CID triaxial tests, although less satisfactory agreement was observed in the case of the specimen associated with negative state parameters.

The TSF construction simulation comprised 34 stages, after which the η / M contours indicated that the areas closer to the toe are prone to static liquefaction, especially when saturated. Therefore, although no significant displacements were observed in the model, the dam was in a state of high mobilization in certain areas and may undergo drastic deformations in the event of a trigger.

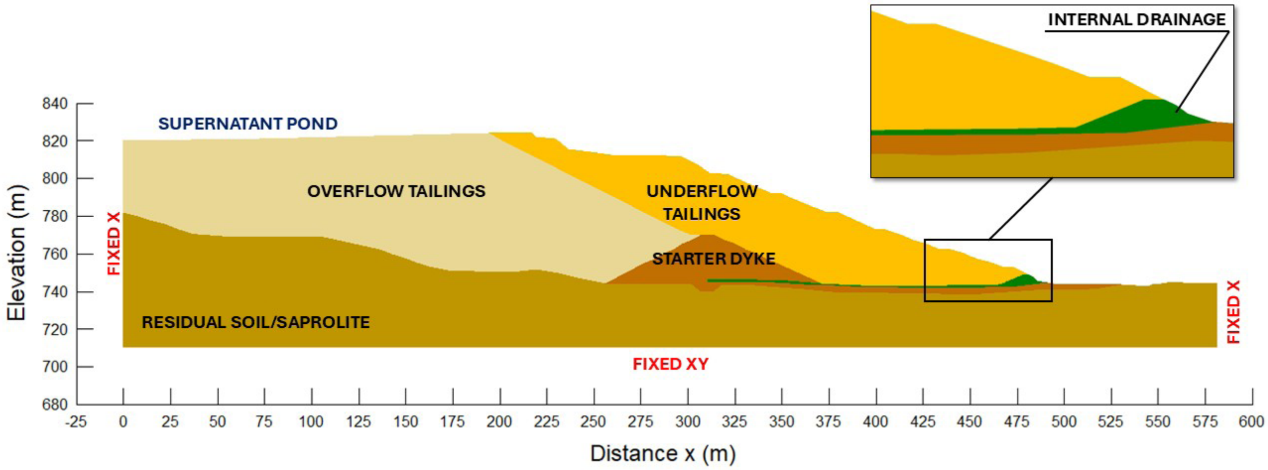

Figure 13. Cross-section of the tailings dam (Coutinho et al., 2025).

Table 2. NorSand parameters for iron ore tailings (Coutinho et al., 2025).

Material	OCR	γ (kN/m^3)	ν	G_{ref} (MPa)	σ_{ref} (MPa)	m	M	N	χ	H_0	H_Ψ
Underflow and overflow tailings	1.00	22.0	0.33	60.0	100.0	0.45	1.34	0.31	4.00	102	346

OCR – Overcosolidation ratio; γ – Specific weight of the material; ν – Poisson's ratio; G_{ref} – Shear modulus at reference stress; σ_{ref} – Normal reference stress; m – Exponent of the reference shear modulus; M – Critical state friction ratio; N – Volumetric coupling in stress dilatancy; χ – Dilatancy constant; H_0 and H_Ψ – Constants for adjusting the plastic hardening modulus.

The critical clogging scenario resulted in the destabilization of the downstream toe of the slope, represented by high η / M values and significant displacements in this area, but without causing complete liquefaction of the entire dam. This condition was achieved only after removing the unstable portion of the dam toe to simulate progressive failure (Figure 14). The NorSand model was able to satisfactorily represent the destabilizing effect of the loss of confinement. These results highlight the importance of recognizing the permeability reduction of the internal drainage due to clogging as a factor that can lead to a TSF failure. In iron ore tailings dams, this reduction can be caused by ochre since the iron concentration creates a propitious environment for ferrobacterial proliferation. The results also describe the role of loss of confinement as a trigger for static liquefaction, which can be the last phase of a progressive rupture.

4. Filtered tailings stacks

4.1 Introduction

Filtered tailings stacks have gained increased attention due to advancements in cost-efficient filtration methods and growing scarcity of water in arid regions (Amoah et al., 2018). High-density thickened and filtered tailings are being increasingly explored as a solution to mitigate both failure risks and the competing demands for water resources (Fourie et al., 2022).

The mining industry has increasingly adopted filtered tailings stacks as an alternative to conventional slurry tailings storage due to heightened safety concerns following major tailings dam failures. Filtered tailings, where solids content exceeds 80%, are stacked in layers to minimize environmental risks such as water contamination and dam collapse. While filtered stack tailings reduce the reliance on large volumes of water and provide greater land efficiency, they also present challenges in achieving optimal compaction during stacking (Davies, 2011). Compaction plays a crucial role in enhancing the stability of filtered stack tailings facilities. Insufficient compaction can render the structure susceptible to liquefaction under certain stress conditions, potentially compromising the stability of the dam (Jefferies & Been, 2015).

High production rates and the Brazilian wet climate pose notable challenges for designers and operators when implementing filtered tailings facilities, which can lead to tailings saturation and increased liquefaction potential.

4.2 Influence of compaction on liquefaction potential in filtered tailings stacks

Andrade et al. (2025) investigated the relationship between compaction levels and the susceptibility to static

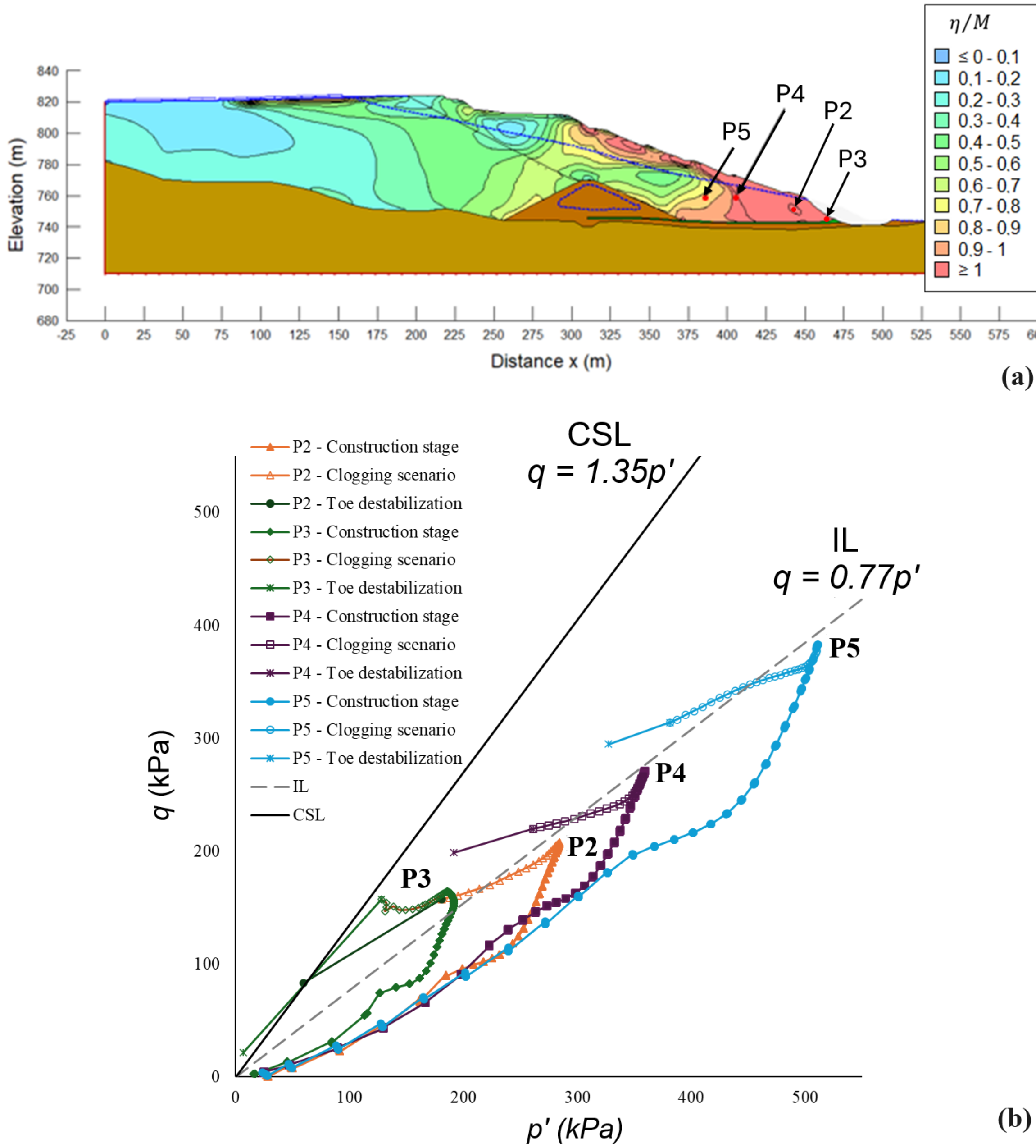

Figure 14. (a) Isovalues of η/M and (b) stress paths in nodes P2, P3, P4 and P5 after the toe break (Coutinho et al., 2025).

liquefaction in a filtered tailings stacks facility based on results of extensive laboratory tests. The study examined the behavior of filtered tailings, focusing on their susceptibility to static liquefaction based on different levels of compaction. Laboratory tests were conducted on both undisturbed and laboratory-compacted samples from a test embankment, shown in Figure 15, composed of three layers with varying thicknesses: 0.60 m, 1.00 m, and 2.00 m (see Figure 15a). These layers were compacted using non-conventional methods, such as bulldozers and trucks, instead of traditional compaction rollers. The undisturbed samples were collected from these three layers. The laboratory-compacted samples were prepared from a tailings batch collected directly from the test embankment.

Key laboratory tests included isotropically consolidated drained (CID), and undrained (CIU) triaxial compression tests performed on samples from different layers of the embankment. Figure 16 illustrates the end points of twenty tests that reached the critical state in both the $q:p'$ and $e:\ln p'$ plots.

The $q:p'$ plane (Figure 16a) provides the slope of a unique CSL given by a critical state friction ratio M_{tc} equal to 1.25, within the range observed by Torres-Cruz & Santamarina (2020). However, the points in the $e:\ln p'$

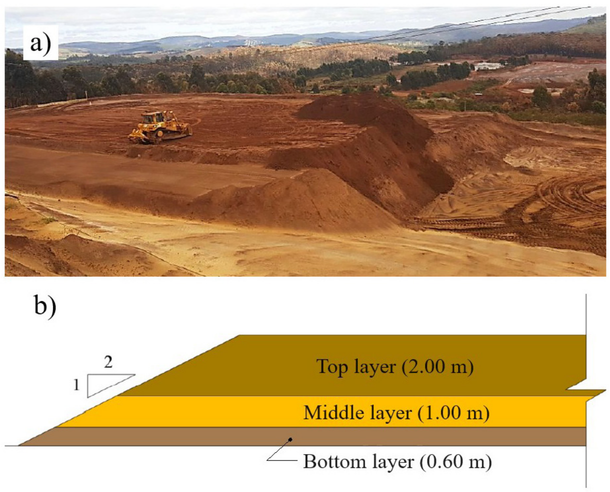

Figure 15. (a) view and (b) cross-section of the test embankment (Andrade et al., 2025).

plot do not describe a single CSL, although the samples used in triaxial tests had similar grain size distributions, which suggests an apparent transitional soil behavior (Coop, 2015). The power law proposed by Li & Wang (1998) was determined for non-linear CSL (Equation 5).

$$e_{cs} = e_{0,ref} - \lambda' \left(p' / p'_{ref} \right)^{\xi} \tag{5}$$

where e_{cs} is the void ratio in the critical state, the reference effective stress (p'_{ref}) adopted (100 kPa) and initial reference void ratio ($e_{0,ref}$), Adjustment parameter for nonlinear CSL in the $e : \ln p'$ plot (λ') and the adjustment parameters for nonlinear CSL in the $e : \ln p'$ plot (ξ). Thus, three CSLs were determined (Figure 16b), each representing the material at 75%, 85% and 95% DC, respectively.

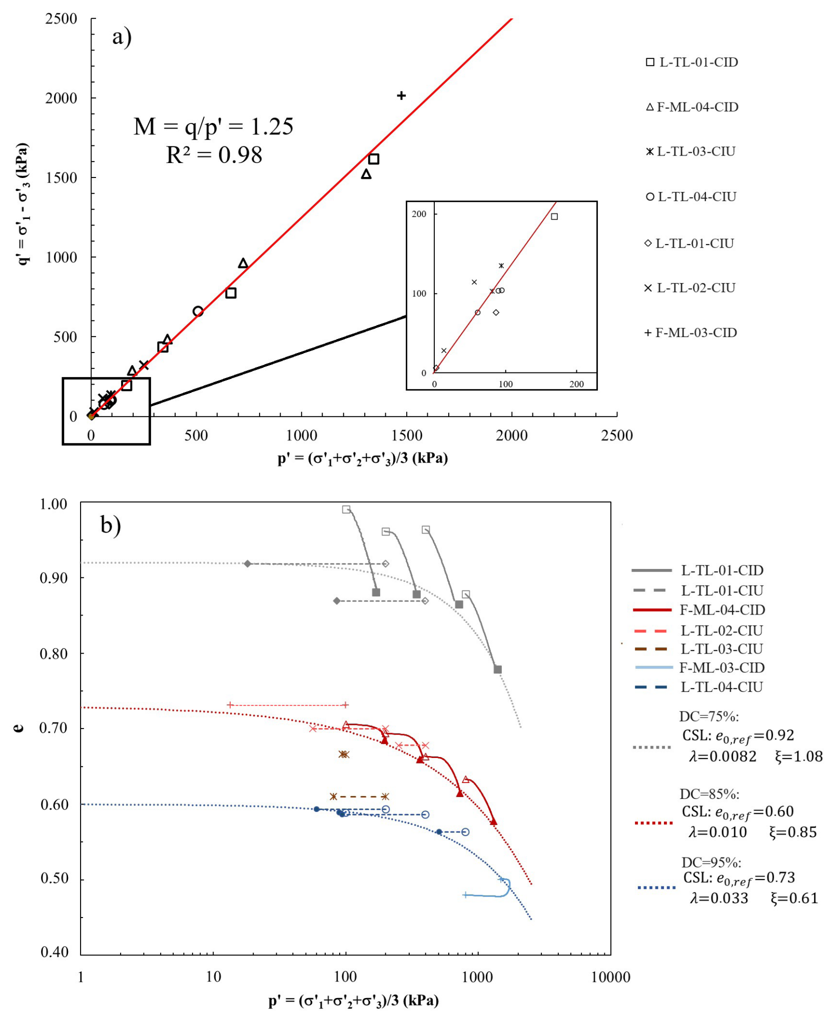

Figure 16. Critical state line in (a) $q : p'$ and (b) $e : \ln p'$ plots (Andrade et al., 2025).

Andrade et al. (2025) identified that samples with degrees of compaction below 90% exhibited a significant reduction in undrained shear strength, making them prone to liquefaction. In-situ measurements showed that the middle and top layers, which had greater thicknesses, had lower degrees of compaction compared to the bottom layer, being more vulnerable to liquefaction. In this regard, thicker layers, while beneficial for productivity, adversely affected compaction efficiency, since they are related to lower degrees of compaction, which in turn increased the tailings' contractive tendencies under undrained conditions. It is important to point out that the susceptibility to liquefaction also depends on the degree of saturation of the tailings (Wang et al., 2024).

Instability lines (ILs) were established, illustrating the relationship between compaction and the tendency to liquefy, as shown in Figure 17. The instability lines demonstrate how compaction levels affect the tailings' behavior. The slope of the instability lines decreased with lower compaction, indicating that these samples were more prone to liquefaction. The study found that samples with a degree of compaction below 85% had the highest susceptibility to liquefaction specifically under low confining stresses. The I_{BU} was also used to quantify the extent of shear strength loss in undrained conditions. Samples with low compaction and low confining pressures were the most susceptible to significant reductions in shear strength. This highlights the importance of achieving optimal compaction to prevent liquefaction (Lade & Yamamuro, 2011) and lesser runout in case of breach.

The results of this study provide key insights into the compaction behavior of filtered tailings, emphasizing the critical role that proper compaction plays in maintaining the stability of tailings facilities. Compaction directly influences the tailings' geotechnical behavior, and failure to meet optimal compaction levels can result in liquefaction risks, particularly in the upper layers of the stack where compaction tends to be lower. These results align with previous studies that also demonstrated that compaction reduces the susceptibility of tailings to liquefaction (Jefferies & Been, 2015; Lade & Yamamuro, 2011).

The study provides evidence that inadequate compaction of filtered tailings stack facilities significantly increases the risk of liquefaction. Even though filtered tailings stack facilities are considered safer than traditional tailings dams, their stability depends on achieving sufficient compaction. Samples with less than 90% compaction exhibited contractive behavior and a substantial loss of undrained shear strength. This work emphasizes the importance of stringent compaction control in filtered tailings stacks construction. More understanding is needed regarding the behavior of filtered tailings stacks under different compaction conditions, and future research should focus on developing improved methods for achieving uniform compaction.

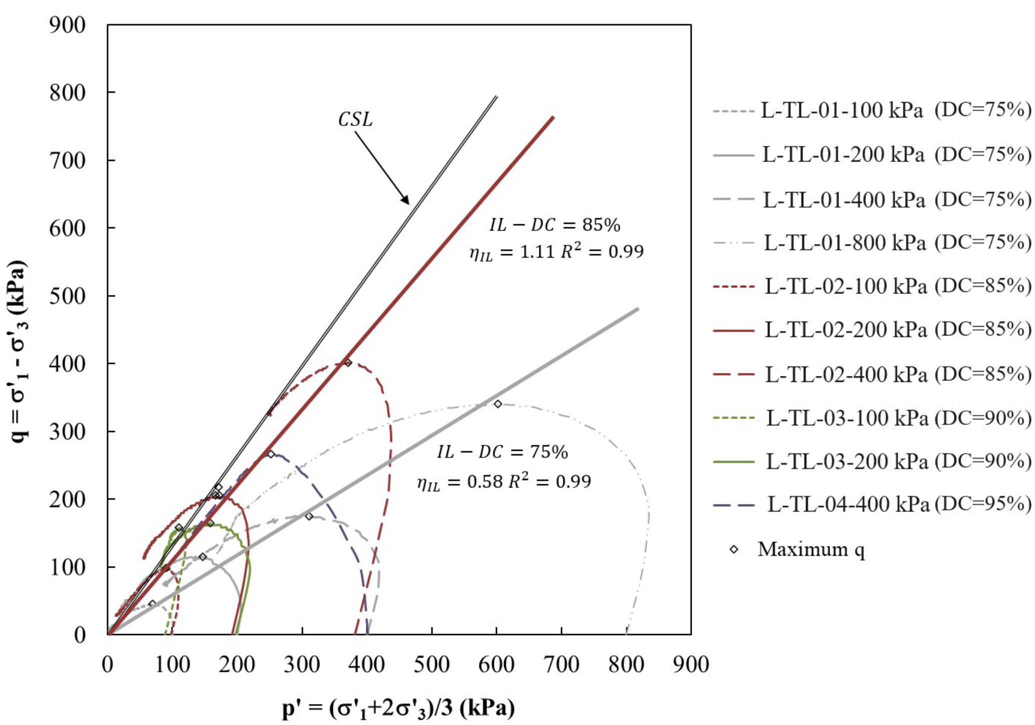

Figure 17. Instability Lines Based on Degree of Compaction (Andrade et al., 2025).

4.3 Static liquefaction susceptibility analysis of a rare earth filtered tailings stack

In the context of energy transition scenario, rare earth elements (REEs), a group of elements that includes the lanthanide metals along with scandium and yttrium, play an important role as raw materials for industry, as REE oxides and metals are associated with applications such as superconductors, miniaturized magnets, catalysts used in refining various products, and components for hybrid vehicles (Lucy, 2015).

Oliveira (2025) studied the key aspects of a REE tailings stack structure, along with a geotechnical characterization of the tailings material and an interpretation of both drained and undrained triaxial tests in the light of the Critical State Soil Mechanics (CSSM).

The rare earth elements at the site are found within ionic clay deposits. The weak bond between the REE and the clay particles facilitates ion exchange using salt, enabling an extraction process involving screening, leaching, precipitation, and filtration. As a result of the initial screening, two distinct types of tailings are produced:

- Undersize: Finer tailings generated during the screening stage, representing 65% of the tailings and subsequently processed through filtration;
- Oversize: Coarser tailings retained during the sieving process.

Since the stack is predominantly composed of undersize tailings, this study focuses on the geomechanical behavior of this material.

The filtered tailings stack in this case study is in the central-western region of Brazil. The construction is planned to occur over six years by the downstream method (Figure 18), reaching a maximum height of approximately 90 meters. The construction will be divided into two zones based on the local rainfall regime. The annual precipitation in the region is approximately 1,500 mm, distributed, mainly, between the months of October and March.

The undersize from the pilot plant underwent an extensive laboratory campaign aimed at characterizing the material and determining its geomechanical properties. This characterization included tests to assess grain size distribution, Atterberg limits, specific gravity, and mineralogy.

Both isotropically consolidated drained (CID) and consolidated undrained (CIU) triaxial tests were conducted with effective confining stresses in the range 100 kPa to 2,200 kPa on samples that were moist tamped to achieve maximum dry densities between 85% and 100% of the Standard Proctor, representing the expected in-situ conditions in different zones of the stack. The results of the triaxial tests were screened to select those that achieved the critical state condition. Of the 40 triaxial tests conducted, only 11 were found suitable for this study. The main data from these tests are summarized in Table 3. Further details regarding the critical state condition will be discussed later on.

The triaxial tests were performed in commercial laboratories, where specimen saturation was achieved through backpressure application and CO_2 percolation, resulting in a minimum Skempton B parameter of 0.95. A freezing technique was used at the end of the shearing to determine the final void ratio. Enlarged and lubricated bases were not utilized in the testing procedures.

The undersize is classified as a non-plastic silty sand (ML), with a specific gravity (G_s) of 2.70. Sub-samples were analyzed using X-ray diffraction (XRD) with the reference intensity ratio (RIR) method for mineral assessment. The undersize is composed of kaolinite (60%), feldspar (15%), mica (14%), and quartz (11%).

Figure 19 compares the grain size distribution of the tailings studied in this work with those reported in Brazilian literature. Unlike other tailings, the undersize shows a well-graded distribution with higher proportions of medium and coarse sand.

The specific gravity found in this study is significantly lower than that of other tailings evaluated. This variation and

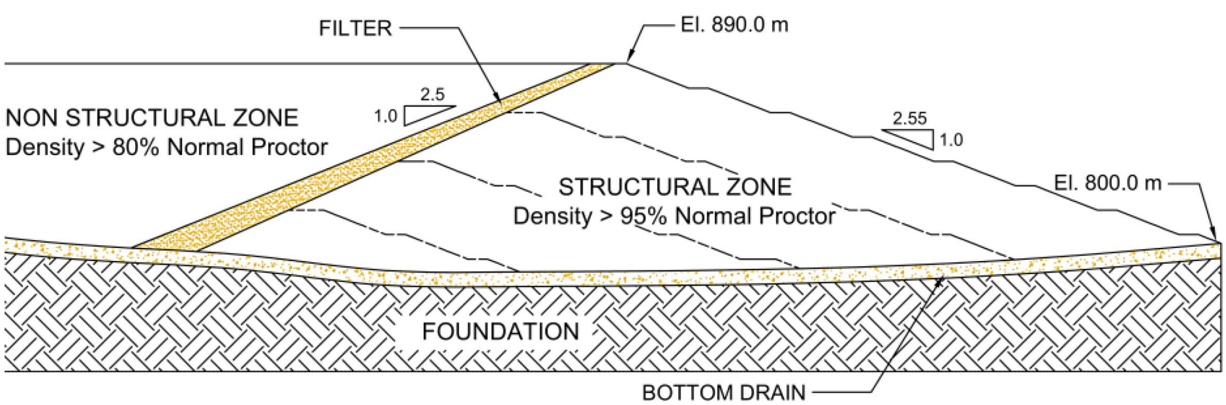

Figure 18. Schematic cross-section of the filtered tailings stack (Oliveira, 2025).

Table 3. Summary of triaxial compression tests data of the undersize tailings (Oliveira, 2025).

ID	Type	DC	$p_0^{'}$ (kPa)	e_{mold}	e_0	ψ_0
1U	CID	85%	100	0.939	0.806	0.09
2U	CIU		300	0.944	0.719	0.11
3U	CID	90%	300	0.831	0.737	0.13
4U	CIU		300	0.826	0.700	0.09
5U	CID		1200	0.835	0.608	0.13
6U	CID	95%	100	0.745	0.672	-0.05
7U	CIU		100	0.749		-0.03
8U	CIU		1200	0.752	0.491	0.02
9U	CID	100%	600	0.654	0.626	0.09
10U	CIU		100	0.661	0.612	-0.10
11U	CIU		2200	0.656	0.362	-0.05

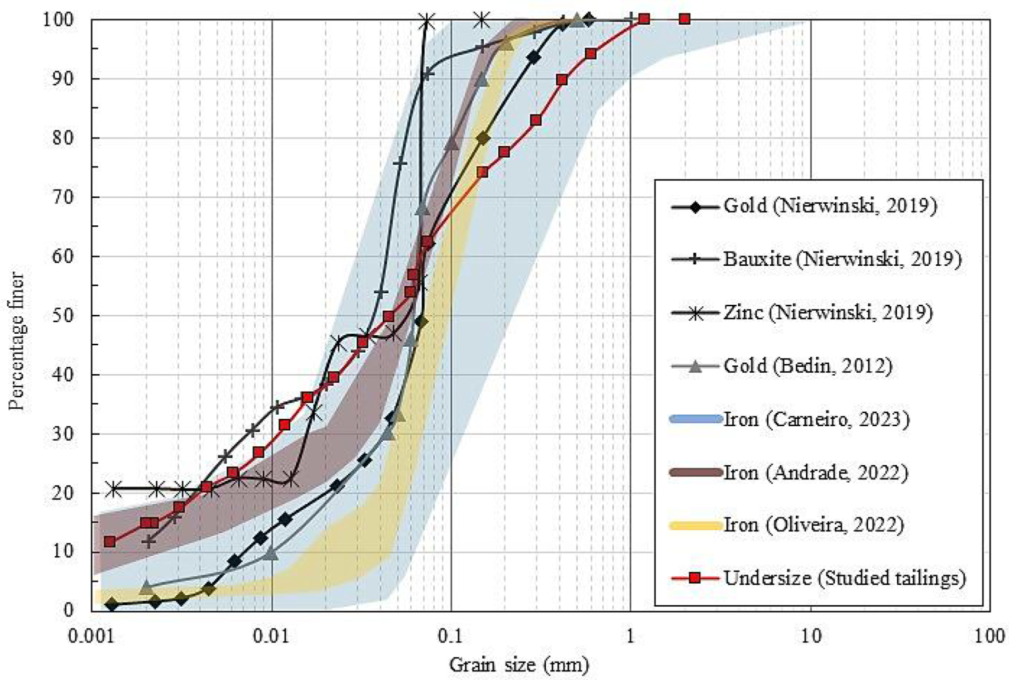

Figure 19. Grain size distribution of rare earth tailings in comparison with different tailings on literature (Oliveira, 2025).

the observed values can be primarily attributed to mineralogy, particularly its low iron content. The mica content is also significant.

The drained tests on the undersize tailings, represented by dashed lines in Figure 20, exhibited contractive behavior, characterized by volume reduction during shearing. Samples 6U and 9U displayed a slight peak in deviatoric stress at approximately 10% axial strain, followed by a decrease in strength at higher strains. Notably, these samples did not exhibit volumetric expansion, which is typically associated with peak strength in dense soils under drained conditions. In the undrained tests, represented by continuous lines, most samples demonstrated positive excess pore pressures and contractive behavior. An exception was observed in the 10U sample, which, being initially dense and subjected to low confining stresses, exhibited initial contraction followed by dilation. To enhance clarity, the results have been stress-normalized due to the wide range of confining stresses tested.

The CSL in the ($e : \ln p'$) plane was defined based on the final void ratio (e_{cs}) and the mean effective stress ($p_{cs}^{'}$) of the triaxial tests in which the critical state was reached. The logarithmic relationship (Equation 6) provided the best fit for the data points.

$$e = \Gamma - \lambda \ln p' \tag{6}$$

A unique CSL was defined as fitted undersize tailings regardless of their initial void ratio and compaction's energy, as shown in Figure 20b. The CSL parameters are $\lambda = 0.098$ and $\Gamma = 1.17$. In the $q : p'$ plot, the CSL resulted in a ratio of $(q_{cs} / p'_{cs}) = 1.16$, corresponding to a critical state friction angle of $\phi'_{cs} = 29°$.

The initial state parameter (ψ_0) was calculated (Table 3) based on the CSL. Negative ψ_0 values, which indicate a tendency for dilative behavior, were observed exclusively in specimens initially compacted with an energy level equal to or greater than 95% of the Standard Proctor. ψ ranged from 0.09 to 0.11 for the specimens compacted DC = 85%, and from –0.04 to 0.02 in denser specimens compacted at DC = 95%.

Triaxial tests revealed predominantly contractive behavior, characterized by volume reduction and the generation of positive pore pressures during shear. Despite this, the material exhibited low brittleness, and no liquefaction was observed, even in specimens with low degrees of compaction subjected to high confining stresses. This behavior may be associated with the high mica content in the tailings, a factor that will be thoroughly investigated in future studies. These tailings also demonstrate remarkably high compressibility for silty sand. At a 90% degree of compaction (*DC*), for instance, they exhibit more than three times the compressibility of the well-documented sand tailings from the Fundão dam, when evaluated at similar void ratios and within a comparable stress range. This high compressibility results in significant volume reduction during consolidation, leading to a lower void ratio prior to shearing and limiting strength loss during undrained loading.

The results of the triaxial tests indicate that the filtered tailings stack of rare earth under investigation are, apparently, not susceptible to liquefaction. The scarcity of studies on rare earth tailings and their geotechnical properties in the existing literature underscores the significance of this work, while simultaneously limiting opportunities for direct comparison. Further field and laboratory investigations under realistic conditions of compaction, loading, and in-situ drainage are

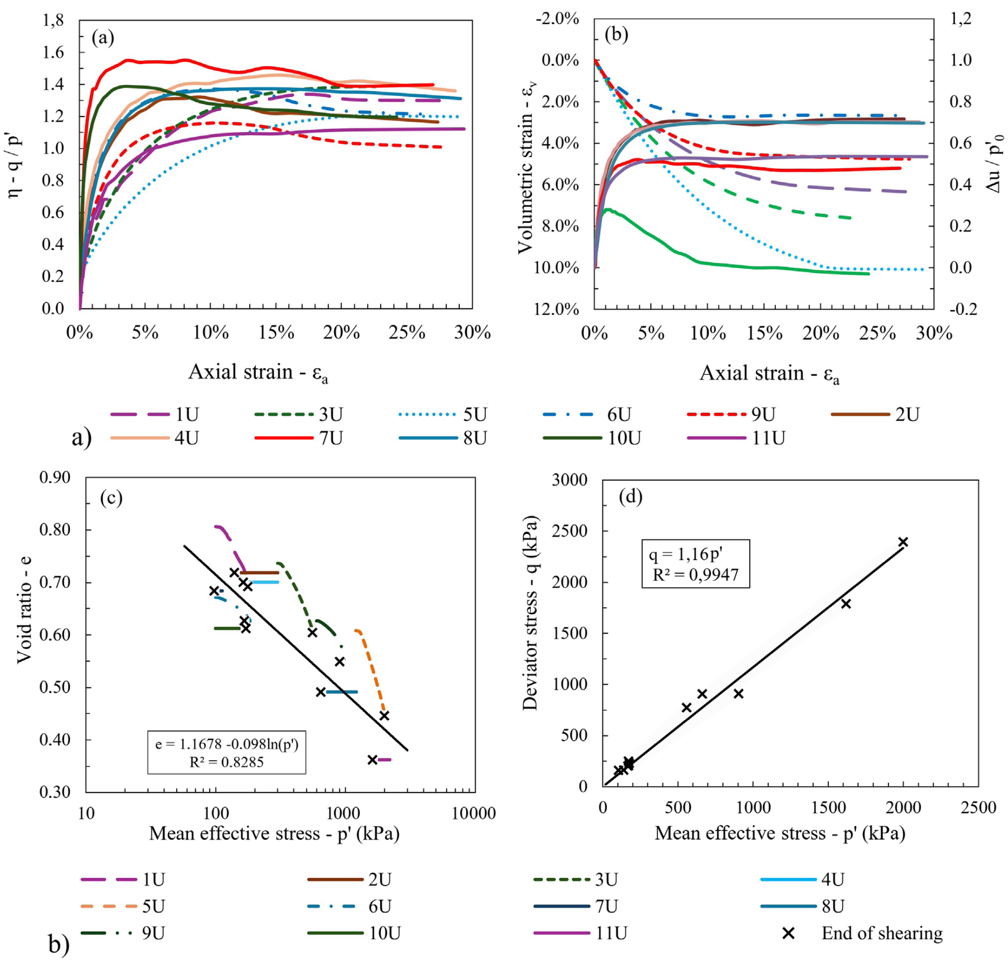

Figure 20. Triaxial tests results: (a) η versus axial strain and (b) critical state line (Oliveira, 2025).

essential to achieve a more comprehensive understanding of this rare earth filtered stack behavior.

4.4 Filtered stacking disposal

Given the hundreds of meters height expected for this TSF type, several studies have focused on the behavior of tailings under very high-stress levels (Delgado et al., 2023; Wagner et al., 2024b; Consoli et al., 2024a; Silva et al., 2023, 2024). For high-stress levels, eventually, it was possible to verify an increase in the non-linearity of CSL in the $e - \log p$' plane, which may be associated with particle breakage or with a relevant morphological particles' evolution (Figure 21a) (Schnaid et al., 2013; Soares & Viana da Fonseca, 2016). Other authors have also observed transitional behavior, characterized by non-unique (straight or curved) CSL (Figure 21b), their locations being highly dependent on the e_0 (Velten et al., 2024) mainly for mixed grading and structured soils and less common for mining tailings. A more detailed investigation at the microstructural level (at particles level) can contribute to the understanding both the non-linearity of CSL and the possible transitional behavior.

Viana da Fonseca et al. (2022) showed a relevant non-linearity of CSL in the $e - \log p$' plane at higher stress levels for the iron ore tailings from Brumadinho reservoir. This non-linearity was related by the authors to the material grading changes by morphological particles' evolution. This evolution behavior was verified for initial mean effective stress higher than 800 kPa.

The CSL slope changes at higher stress level, associated with increased grain angularity have also been reported by Soares & Viana da Fonseca (2016). Further research, by quantification of morphological changes during laboratory tests and discrete element method (DEM) simulations, could help to validate this stress-strain behavior at macro-scale.

Delgado et al. (2023) have highlighted, through drained triaxial tests on sandy-silty iron ore tailings from Brazilian Iron Quadrangle region, that from about 3.200 kPa of mean effective stress, some relevant level of particle breakage appears to occur during shearing. This particle breakage under high stress levels increases the fines content, consequently, changing the grain size distribution of the material. Oliveira et al. (2025) observed that the fines introduction conditioned a downward translation in the CSL in the $e - p$' plane. Wagner et al. (2024a) observed that, when fines content exceeds a certain limit, the fines begin to regulate the mechanical behavior of the material, and the CSL can assume a position in the $e - p$' plane superior to its original position (before the fines introduction).

Consoli et al. (2023), aiming to generalize the behavior of the sandy-silty iron ore tailings from Brazilian Iron Quadrangle region, showed, after drained triaxial tests under mean effective stresses up to 120 MPa, that particle breakage caused by high-stress levels exerts an important influence on the mechanical behavior, evidenced by the curvature of the CSL in the $v - \ln p'$ plane. The authors proposed an equation with five parameters, which describes a curve as an 'inverted S' shape (Figure 22), as an alternative to representing the CSL in the $v - \ln p'$ plane. In this equation, v_0 is the limiting (maximum specific volume at critical state that the material could achieve) specific volume; v_{min} is the inferior asymptote, related to the minimum specific volume that the material could achieve; C_1, C_2, and C_3 are fitted to match laboratory test results that for the silty sandy iron ore tailings studied by the authors are respectively: -0.974, -0.074, and 2.126. The parameter p'_{ref} is herein assumed

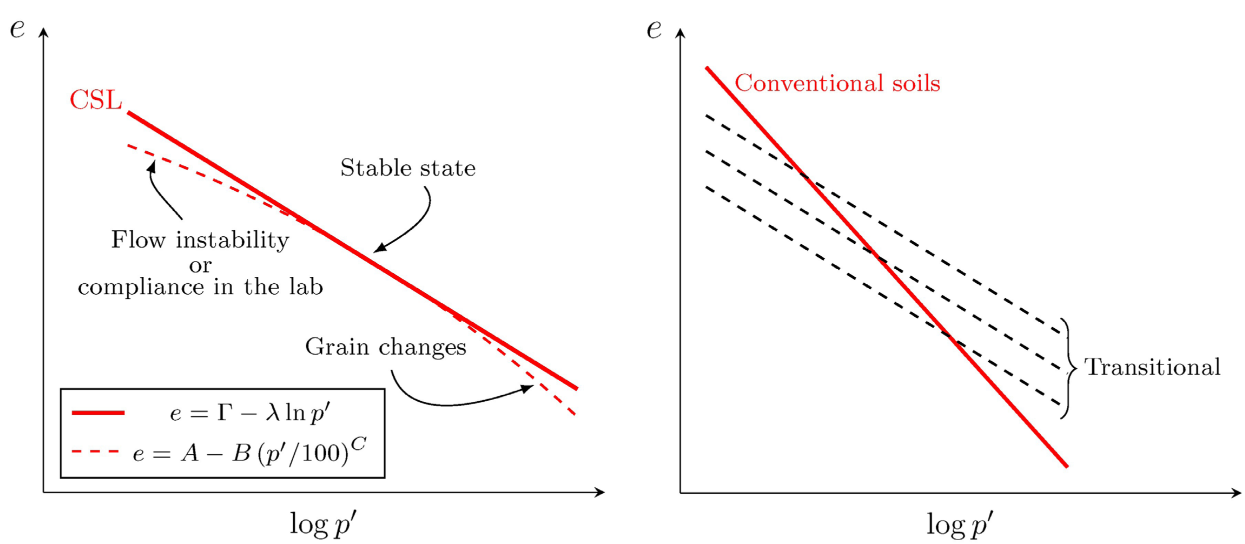

Figure 21. Schematic illustration of (a) non-linearity of CSL and (b) the transitional soil behaviour (modified from Viana da Fonseca et al., 2021).

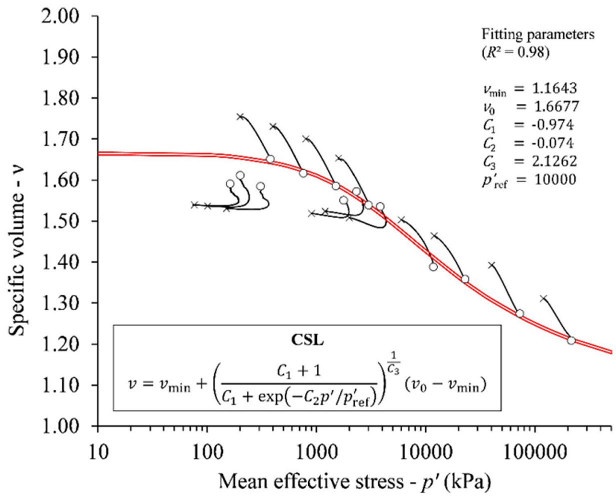

Figure 22. Proposed 'inverted S' shape CSL in v – ln p' plane (Consoli et al., 2023).

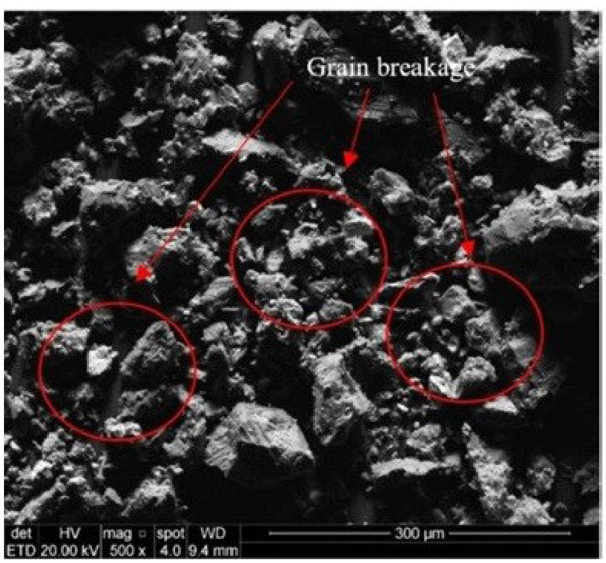

Figure 23. Scanning Electron Microscopy image at 500x magnification of iron ore tailings after triaxial testing with a confining stress of 3 MPa (Mafessoli et al., 2023).

as 10 MPa. This 'S-shaped' CSL proved to be equally favorable for analyzing the critical state behavior of lightly cemented compacted iron ore under high confining pressures, facilitating its incorporation in modeling to predict their mechanical behavior (Consoli et al., 2024b). Nevertheless, it is emphasized that such a model based on 'inverted S' shape CSL is not yet a consensus and should be evaluated with caution, as it can be influenced by spurious localized rupture structures (shear bands).

Also, regarding filtered tailings stacks, Nadai et al. (2023) addressed aspects related to the dynamics of water flow inside these structures, particularly the concerns about the formation of saturated regions due to capillarity, including those due to local climatic conditions. It was observed that studying the hydraulic characteristics of mixtures between plastic and coarse tailings is a way of increasing the efficiency of stack designs. Jesus et al. (2023) studied the characteristics of mining tailings in the unsaturated condition, using the model proposed by Vilar (2006). According to these authors, the model was suitable for determining the failure envelope of an iron ore tailings from the Brazilian Iron Quadrangle in the unsaturated condition.

Consoli et al. (2022) highlighted that stacking filtered tailings improved with Portland cement in compacted layers is a way of making stacks with steeper slopes feasible, covering smaller areas, and promoting lower environmental impacts. Mafessoli et al. (2023) showed that the voids/cement factor proposed by Consoli et al. (2007) for natural and artificially cemented soils is suitable for estimating the unconfined compression strength and initial stiffness of iron ore tailings stabilized with Portland cement. The addition of the cementing agent increased both the mechanical strength and stiffness of the composite material and led to a transition from purely frictional behavior to cohesive-frictional behavior. Meanwhile, the high stress levels to which these materials can be subjected, especially at the base of high filtered tailings stacks, can cause the failure of the bonds. Figure 23 shows an example of a Portland cement-stabilized iron ore tailings sample subjected to a triaxial test with a confining stress of 3 MPa, at which point the grains and cement bonds broke.

In addition to evaluating the use of Portland cement, other types of cementing agents, such as alkali-activated cements, have been considered (Bastos et al., 2016; Consoli et al., 2018; Bruschi et al., 2022; Santos et al., 2022; Servi et al., 2022; Caetano et al., 2023; Levandoski et al., 2023). Farenzena et al. (2024) studied the effects of stabilizing filtered iron ore tailings by adding an alkali-activated cement composed of two by-products of iron ore processing, metakaolin and sodium silicate. The formation of bonds was found to induce cohesive-frictional behavior in the material, which contributes to increasing mechanical strength. The authors emphasize that alkali-activated cements, in addition to their environmental benefits, are less expensive than conventional cementing agents such as Portland cement and lime. Furthermore, the stabilization of mining tailings can also be carried out using polymers (Carneiro & Dal Toé Casagrande, 2020). Alelvan et al. (2022a) investigated the feasibility of using polymers to improve the characteristics of silty gold ore tailings and demonstrated that polymers are an interesting alternative to promote increased cohesion between grains, to produce a composite with greater mechanical strength.

5. Concluding remarks

From an engineering standpoint, the disposal of tailings in dams and filtered stacks presents a significant ongoing challenge that must be addressed to manage the massive volumes of material produced annually by mining operations. Among the largest earth structures in the world, Tailings Storage Facilities (TSFs) have received intense regulatory examination following recent global failures, prompting scientific research advancements, collection of datasets, and investigation of case studies to enhance our understanding of their design and performance.

Some of the recent contributions from Brazilian research groups are addressed in this paper. Considering the primary concern surrounding liquefaction dam failures, focus has been directed towards assessing constitutive parameters from laboratory tests such as triaxial and hollow cylinder in both compression and extension. Additionally, a critical evaluation is provided on modelling the strain softening behaviour in non-plastic tailings under various loading conditions. The strength of plastic tailings was evaluated, with particular emphasis on their low undrained strength ratio, in comparison to non-plastic tailings. A final word of caution goes towards the indiscriminate use of moist tamped specimens to investigate the hydraulic-placed soils such as tailings. Recent studies (Hight, 2013) show that moist tamping may result in non-uniform void distribution with the exaggerated presence of macro-voids, leading also to large collapse potential.

Recently, filtered stacks are increasingly viewed as a preferable option for tailings storage for several reasons, including their stability and structural integrity combined to the lower risk of catastrophic failure. However, the design of filtered stacks presents several challenges, including the variability of tailings, their transitional behavior, the susceptibility to liquefaction of undercompacted materials, and the effects of particle breakage, among other factors described in the paper. This paper has highlighted several aspects related to the behavior of tailings, including the prediction of their properties and the related to modeling and design challenges.

Acknowledgements

The authors would like to thank the Brazilian Federal Agency for Support and Evaluation of Graduate Education (CAPES), Brazilian National Council for Scientific and Technological Development (CNPq), Carlos Chagas Filho Foundation for Research Support in the State of Rio de Janeiro (FAPERJ) for provide financial support.

Declaration of interest

The authors have no conflicts of interest to declare. All co-authors have observed and affirmed the contents of the paper and there is no financial interest to report.

Authors' contributions

Márcio de Souza Soares de Almeida: conceptualization, data curation, methodology, resources, supervision, validation, visualization, writing – original draft. Fernando Schnaid: data curation, validation, visualization, writing – original draft. Romário Stéffano Amaro da Silva: data curation, validation, visualization, writing – original draft. Leonardo De Bona Becker: data curation, validation, visualization, writing – original draft. Bruno Guimarães Delgado: data curation, validation, visualization, writing – original draft. Antonio Jeronimo Pereira de Souza Junior: data curation, validation, visualization, writing – original draft. Frederico Wagner Alvarenga Oliveira: data curation, validation, visualization, writing – original draft. Maria do Carmo Reis Cavalcanti: data curation, validation, visualization, writing – original draft. Sparsha Sinduri Nagula: data curation, validation, visualization, writing – original draft.

Data availability

No dataset was generated or evaluated in the course of the current study; therefore, data sharing is not applicable.

Declaration of use of generative artificial intelligence

This work was prepared without the assistance of any generative artificial intelligence (GenAI) tools or services. All aspects of the manuscript were developed solely by the authors, who take full responsibility for the content of this publication.

List of symbols and abbreviations

b	Intermediate stress ratio
e	Void ratio
e_0	Post-consolidation void ratio
$e_{0,ref}$	Reference void ratio
e_{cs}	Critical state void ratio
k	Permeability coefficient
m	Exponent of the reference shear modulus
p'	Mean effective stress
p'_0	Consolidation mean effective stress
p'_{cs}	Mean effective stress at the critical state
p'_{ref}	Reference mean effective stress
q	Deviator stress
q_t	Corrected cone resistance
$s_{u,liq}$	Liquified undrained strength
$s_{u,peak}$	Peak undrained strength
t	Time
CASM	Clay and Sand Model
CAU	Consolidated anisotropically undrained
CID	Consolidated isotropically drained
CIU	Consolidated isotropically undrained
CPTu	Cone penetration test with pore pressure measurement
CSD	Constant Shear Drained
CSL	Critical State Line

CSSM Critical State Soil Mechanics
D_{min} Minimum dilatancy
DC Degree of compaction
FST Fundão sand tailings
G_0 Small strain shear modulus
G_{ref} Shear modulus at reference stress
G_s Specific gravity of particles
H Plastic hardening modulus
H_0 Constant for adjusting the plastic hardening modulus
H_ψ Constant for adjusting the plastic hardening modulus
HC Hollow cylinder test
I_{BU} Brittleness index
I_c Soil Behavior Classification index
IL Instability line
LE Lateral extrusion
M Critical state friction ratio
M_{tc} Critical state friction ratio obtained from triaxial compression
N Volumetric coupling in stress dilatancy
N_{kt} Cone factor
Q_{tn} Normalized cone tip resistance
REE Rare earth elements
SFS Silica fine sands
TDF Tailings Disposal Facilities
TSF Tailings Storage Facility
TX Triaxial test
XRD X-ray diffraction
α Principal stress angle
γ Unit weight
$\delta \varepsilon_a$ Axial strain increment
δt Time increment
ε_a Axial strain rate
η Stress ratio q / p'
η_{IL} Instability Line slope
η_{max} Peak stress ratio
λ Slope of the CSL in the e:ln p' plot
ν Poisson's ratio
σ_2 Intermediate principal stress
σ_{ref} Normal reference stress
σ'_{vo} Effective vertical normal stress
χ Dilatancy constant
ψ State parameter
ψ_0 Initial state parameter
Γ Void ratio at reference pressure of 1 kPa
ϕ'_{cs} Critical state friction angle
ϕ'_p Peak friction angle

References

ABNT NBR 13028. (2013). *Mineração: elaboração e apresentação de projeto de barragens para disposição de rejeitos, contenção de sedimentos e reserva de água: requisitos.* Associação Brasileira de Normas Técnicas, Rio de Janeiro.

Agurto-Detzel, H., Bianchi, M., Assumpção, M., Schimmel, M., Collaço, B., Ciardelli, C., Barbosa, J.R., & Calhau, J. (2016). The tailings dam failure of 5 November 2015 in SE Brazil and its preceding seismic sequence. *Geophysical Research Letters*, *43*(10), 4929-4936. http://doi.org/10.1002/2016GL069257.

Ahmadi, M.M., Byrne, P.M., & Campanella, R.G. (2005). Cone tip resistance in sand: modeling, verification, and applications. *Canadian Geotechnical Journal*, *42*(4). https://doi.org/10.1139/t05-030.

Albuquerque Filho, L. H. (2004). *Avaliação do comportamento geotécnico de barragens de rejeitos de minério de ferro através de ensaios de Piezocone* [Dissertação de mestrado]. Universidade Federal de Ouro Preto (in Portuguese).

Alelvan, G.M., Ferreira, J.W.D.S., Dal Toé Casagrande, M., & Consoli, N.C. (2022a). Proposal of new construction material: polymer-stabilized gold ore tailings composite. *Sustainability*, *14*(20), 13648. http://doi.org/10.3390/su142013648.

Almeida, M.S.S. (1982). The undrained behaviour of the Rio de Janeiro clay in the light of Critical State theories. *Soils and Rocks*, *5*(2), 3-24.

Almeida, M.S.S., & Ortigão, J.A.R. (1982). Performance and finite element analyses of a trial embankment on soft clay. In *Proceedings of the International Symposium on Numerical Models in Geomechanics* (pp. 548-558), Zurich.

Amoah, N., Dressel, W., & Fourie, A.B. (2018). Characterization of unsaturated geotechnical properties of filtered magnetite tailings in a dry stack facility. In *Paste 2018: Proceedings of the 21st International Seminar on Paste and Thickened Tailings* (pp. 375-388). Australian Centre for Geomechanics. http://doi.org/10.36487/ACG_rep/1805_31_Amoah.

ANCOLD. (2019). *Planning, design, construction, operation and closure (revision 1)*. Australian National Committee on Large Dams.

Andrade, R.B., Silva, R.S.A., Almeida, M.S.S., & Nagula, S.S. (2025). Evaluation of the liquefaction potential of filtered tailings stacks by means of laboratory investigation. *Canadian Geotechnical Journal*, *62*, 1-13. http://doi.org/10.1139/cgj-2024-0274.

André, I.M.O., Telles, A.C.M., Becker, L.B., & Barbosa, M.C. (2018). Comparação do ângulo de atrito de um rejeito de minério de ferro, no estado de regime permanente, determinado a partir de ensaios triaxial, ring shear, e cisalhamento direto. In *Anais do XIX Congresso Brasileiro de Mecânica dos Solos e Engenharia Geotécnica*, Salvador, BA.

ANM. (2022). *Resolução ANM Nº 95*. Agência Nacional de Mineração, Brasília (in Portuguese).

Araújo, G.S., Gardoni, M.G., & Gomes, R.C. (2010). The behaviour of non-woven geotextiles in tailings dams drainage systems. In *Proceedings of the 9th International Conference on Geosynthetics, Geosynthetics for a Challenging World* (Vol. 3, pp. 1075-1078), Guarujá, SP.

Arroyo, M., & Gens, A. (2021). *Computational analyses of Dam I failure at the Corrego de Feijao mine in Brumadinho: CIMNE report to VALE*. CIMNE International Center for Numerical Methods in Engineering. Retrieved in December 28, 2024, from https://tinyurl.com/4zu8ymeh

Ayala, G.R.L., Cavalcanti, M.D.C.R., & Mahler, C.F. (2020). Análise de estabilidade de talude considerando o efeito sísmico de uma barragem de rejeito de minério de ferro. In *Anais do XX Congresso Brasileiro de Mecânica dos Solos e Engenharia Geotécnica (COBRAMSEG 2020)*, Campinas, SP. http://doi.org/10.4322/cobramseg.2022.0704.

Bastos, L.A.D.C., Silva, G.C., Mendes, J.C., & Peixoto, R.A.F. (2016). Using iron ore tailings from tailing dams as road material. *Journal of Materials in Civil Engineering*, *28*(10), 04016102. http://doi.org/10.1061/(ASCE)MT.1943-5533.0001613.

Becker, L.D.B., Fabre, J.S., & Barbosa, M.C. (2022). Determination of the critical state of a silty sand iron tailings in triaxial extension tests using photographic correction. *Canadian Geotechnical Journal*, *60*(4), 504-520. http://doi.org/10.1139/cgj-2021-0637.

Becker, L.B., Cavalcanti, M., & Marques, A.A.M. (2023a). Statistical analysis of the effective friction angle of sand tailings from Germano Dam. *Infrastructures*, *8*(61), 61. http://doi.org/10.3390/infrastructures8030061.

Becker, L. D. B., Ehrlich, M., & Barbosa, M. C. (2023b). Discussion of "Stability analysis of upstream tailings dam using numerical limit analyses". *Journal of Geotechnical and Geoenvironmental Engineering*, *149*(3), 07023001-1. http://doi.org/10.1061/JGGEFK.GTENG-11272.

Becker, L.D.B., Aguiar, A.L.S.L., & Lacerda, W.A. (2024). Variability of the undrained strength of the plastic tailings from the Germano dam in Mariana, Brazil. *Geomechanics and Geophysics for Geo-Energy and Geo-Resources*, *10*(25), 25. http://doi.org/10.1007/s40948-024-00750-4.

Bedin, J., Schnaid, F., Fonseca, A.V., & Costa Filho, L.D.M. (2012). Gold tailings liquefaction under critical state soil mechanics. *Geotechnique*, *62*(3), 263-267. http://doi.org/10.1680/geot.10.P.037.

Been, K., & Jefferies, M.G. (1985). A state parameter for sands. *Geotechnique*, *35*(2), 99-112. http://doi.org/10.1680/geot.1985.35.2.99.

Bittar, R.J., Gomes, R.C., Melo, L.C.Q.C., & Martins, P.M. (2010). Feasibility studies for phosphate fine tailing disposal in geotextile tubes. In *Proceedings of the 9th International Conference on Geosynthetics, Geosynthetics for a Challenging World* (Vol. 3, pp. 1111-1114), Guarujá, SP.

Bishop, A.W. (1967). Progressive failure with special reference to the mechanism causing it. In *Proceeding of the geotechnical conference* (Vol. 2, pp. 142-150), Oslo.

Bishop, A.W. (1973). The stability of tips and spoil heaps. *Quarterly Journal of Engineering Geology and Hydrogeology*, *6*(3), 335-376. https://doi.org/10.1144/GSL.QJEG.1973.006.03.15.

Brasil. Agência Nacional de Mineração – ANM. (Agosto 12, 2019). Resolução nº 13, de 8 de agosto de 2019. Estabelece medidas regulatórias objetivando assegurar a estabilidade de barragens de mineração. *Diário Oficial [da] República Federativa do Brasil*.

Brien, K.O., Brien, T.O., & Robinson, B. (2021). Using the NorSand constitutive model as a tool in assessing the static and dynamic stability of tailings slopes containing contractive material. In *Proceedings of the 88th Annual Meeting of International Commission on Large Dams – ICOLD*, New Delhi, India.

Bruschi, G.J., Santos, C.P., Levandoski, W.M.K., Ferrazzo, S.T., Korf, E.P., Saldanha, R.B., & Consoli, N.C. (2022). Leaching assessment of cemented bauxite tailings through wetting and drying cycles of durability test. *Environmental Science and Pollution Research International*, *29*(39), 59247-59262. http://doi.org/10.1007/s11356-022-20031-5.

Bruschi, G.J., Santos, C.P.D., Scheuermann Filho, H.C, Silva Martinatto, C., Schulz, L.R., Silva, J.P.D.S., & Consoli, N.C. (2023). Mechanical and microstructural response of iron ore tailings under low and high pressures considering a wide range of molding characteristics. *Mining*, *3*(4), 712-730. http://doi.org/10.3390/mining3040039.

Caetano, I., Rios, S., Fonseca, A.V., & Delgado, B. (2023). Stabilization of iron tailings with alkali-activated binders. In *Proceedings of the 1st International Conference on Geotechnics of Tailings and Mine Waste (1-ICGTMW2023)*, Ouro Preto, Brazil.

Carneiro, A.D.A., & Dal Toé Casagrande, M. (2020). Mechanical and environmental performance of polymer stabilized iron ore tailings. *Soils and Rocks*, *43*(4), 679-689. http://doi.org/10.28927/SR.434679.

Carneiro, J.J.V., Marques, E.A.G., Viana da Fonseca, A.J.P., Ferraz, R.L., & Oliveira, A.H.C. (2023). Characterization of an iron ore tailing sample and the evaluation of its representativeness. *Geotechnical and Geological Engineering*, *41*(5), 2833-2852. http://doi.org/10.1007/s10706-023-02430-8.

Carvalho, J.V.D.A., Wagner, A.C., Scheuermann Filho, H.C., & Consoli, N.C. (2024). The role of fabric, stress history, mineralogy, and particle morphology on the triaxial behavior of nontextbook geomaterials. *Journal of Geotechnical and Geoenvironmental Engineering*, *150*(8), 04024055. http://doi.org/10.1061/JGGEFK.GTENG-12319.

Carvalho, J.V.D.A., Wagner, A.C., Scheuermann Filho, H.C., Chaves, H.M., Silva, J.P.S., Delgado, B.G., & Consoli, N.C. (2023). Evaluation of strength parameters for application in cemented iron ore tailings stacks. *Indian Geotechnical Journal*, *53*(4), 775-788. http://doi.org/10.1007/s40098-023-00712-9.

Cavalcante, A.L., Farias, M.M., & Assis, A.P. (2012). On modeling tailings deposition: analytical and numerical methods. *International Journal of Science and Engineering Investigations*, *1*(7), 64-70.

CDA. (2013). *Dam safety guidelines*. Canadian Dam Association, Ontario.

CDA. (2019). *Application of dam safety guidelines to mining dams.* Canadian Dam Association, Ontario.

Chu, J., Leroueil, S., & Leong, W.K. (2003). Unstable behaviour of sand and its implication for slope instability. *Canadian Geotechnical Journal*, *40*(5), 873-885. http://doi.org/10.1139/t03-039.

Consoli, N.C., Foppa, D., Festugato, L., & Heineck, K.S. (2007). Key parameters for strength control of artificially cemented soils. *Journal of Geotechnical and Geoenvironmental Engineering*, *133*(2), 197-205. http://doi.org/10.1061/(ASCE)1090-0241(2007)133:2(197).

Consoli, N.C., Silva, A.P., Nierwinski, H.P., & Sosnoski, J. (2018). Durability, strength, and stiffness of compacted gold tailings-cement mixes. *Canadian Geotechnical Journal*, *55*(4), 486-494. http://doi.org/10.1139/cgj-2016-0391.

Consoli, N.C., Vogt, J.C., Silva, J.P.S., Chaves, H.M., Scheuermann Filho, H.C., Moreira, E.B., & Lotero, A. (2022). Behaviour of compacted filtered iron ore tailings–Portland cement blends: new Brazilian trend for tailings disposal by stacking. *Applied Sciences*, *12*(2), 836. http://doi.org/10.3390/app12020836.

Consoli, N.C., Azambuja Carvalho, J.V., Wagner, A.C., Scheuermann Filho, H.C., Carvalho, I., Cacciari, P.P., & Silva, J.P.S. (2023). Determination of critical state line (CSL) for silty-sandy iron ore tailings subjected to low-high confining pressures. *Journal of Rock Mechanics and Geotechnical Engineering*. http://doi.org/10.1016/j.jrmge.2023.06.014.

Consoli, N.C., Silva, J.P.S., Wagner, A.C., Carvalho, J.V.D.A., Baudet, B.A., Coop, M.R., Scheuermann Filho, H.C., Carvalho, I., Sousa, G.M., & Cacciari, P.P. (2024a). Critical state analysis of two compacted filtered iron ore tailings with different gradings and mineralogy at different stages of treatment. *Acta Geotechnica*, *19*(2), 881-898. http://doi.org/10.1007/s11440-023-01963-9.

Consoli, N.C., Scheuermann Filho, H.C., Wagner, A.C., Carvalho, J.V.A., Guedes, J.P.C., Carvalho, I., Delgado, B.G., & Silva, J.P.S. (2024b). Insights into the mechanics of uncemented and lightly cemented compacted iron ore tailings under high confining pressures. *Soil and Foundation*, *64*(6), 101543. http://doi.org/10.1016/j.sandf.2024.101543.

Coop, M.R. (2015). Limitations of a critical state framework applied to the behaviour of natural and "transitional" soils. In *6th International Symposium on Deformation Characteristics of Geomaterials* (pp. 115-155), Buenos Aires. http://doi.org/10.3233/978-1-61499-601-9-115.

Costa, F.F.S., Delgado, B.G., & Castilho, B.M. (2024). Numerical sensitivity analysis for stress-strain simulation and flow liquefaction assessment of tailings storage facilities using the NorSand constitutive model. *Soils and Rocks*, *47*(1), 83-97.

Coutinho, R.S. (2022). *Experimental studies and the NorSand model applied to an iron ore tailing* [Master's dissertation]. Federal University of Rio de Janeiro.

Coutinho, R.S., Silva, R.S.A., Almeida, M.S.S., Cavalcanti, M.C.R., Nagula, S.S., & Delgado, B.G. (2025). Static liquefaction susceptibility of Brazilian iron ore tailings dam: combined laboratory testing and numerical modeling approach. *International Journal of Geomechanics*, *25*(8), 04025167. http://doi.org/10.1061/IJGNAI.GMENG-11018.

Davies, M. (2011). Filtered dry stacked tailings: the fundamentals. In *Proceedings of the 15th International Conference on Tailings and Mine Waste*, Vancouver, Canada. http://doi.org/10.14288/1.0107683.

Delgado, B.G., Viana da Fonseca, A., Bittar, R.J., Castilho, B.M., & Coelho, D. (October 24-26, 2023). Geomechanical behaviour of an iron ore tailings under high-stress levels for disposal by dry stacking. In *Proceedings of the 1st International Conference on Geotechnics of Tailings and Mine Waste*, Ouro Preto, Brazil.

Dias Neto, S.L.S., Ferraz, R.L., Silva, T.O., Marques, E.A.G., Pitanga, H.N., & Cândido, E.S. (2024). Hydraulic characteristics of silt-sized iron ore tailings. *Geotechnical and Geological Engineering*, *42*(5), 1-23. http://doi.org/10.1007/s10706-024-02755-y.

Eckersley, D. (1990). Instrumented laboratory flowslides. *Geotechnique*, *40*(3), 489-502. http://doi.org/10.1680/geot.1990.40.3.489.

Espósito, T., Assis, A., & Giovannini, M. (2002). Influence of the variability of geotechnical parameters on the liquefaction potential of tailing dams. *International Journal of Surface Mining. Reclamation and Environment*, *16*(4), 304-313. http://doi.org/10.1076/ijsm.16.4.304.8639.

Fanni, R., Reid, D., & Fourie, A. (2024). Effect of principal stress direction on the instability of sand under the constant shear drained stress path. *Geotechnique*, *74*(9), 875-891. http://doi.org/10.1680/jgeot.22.00062.

Farenzena, H.P., Bruschi, G.J., Schmitt Medina, G., Sousa Silva, J.P., Lotero, A., & Consoli, N.C. (2024). Iron ore tailings stabilization with alternative alkali-activated cement for dry stacking: mechanical and microstructural insights. *Canadian Geotechnical Journal*, *61*(4), 649-667. http://doi.org/10.1139/cgj-2023-0125.

Faria, A.D.O., Delgado, B.G., Ferreira, L.D., & Santos, M.P.D. (2023). Comparative evaluation of constitutive models for stress-strain analysis of an iron ore tailings from the Quadrilátero Ferrífero, Minas Gerais, Brazil. *Soils and Rocks*, *47*(1), e2024011022. http://doi.org/10.28927/SR.2024.011022.

Faria, A., Junior, M., Carneiro, J., Dias, M., & Pinto, G. (2024). Evaluation of the susceptibility to flow liquefaction of an iron ore tailings using the state parameter and Yield Stress Ratio approach. In *7th International Conference on Geotechnical and Geophysical Site Characterization (ISC 24)*. Scipedia. http://doi.org/10.23967/isc.2024.193.

Fourie, A., Verdugo, R., Bjelkevik, A., Torres-Cruz, L.A., & Znidarcic, D. (2022). Geotechnics of mine tailings: a 2022 state of the art. In *Proceedings of the 20th International Conference on Soil Mechanics and Geotechnical Engineering.* ICSMGE.

Ghafghazi, M., & Shuttle, D. (2008). Interpretation of sand state from cone penetration resistance. *Geotechnique*, *58*(8), 623-634. http://doi.org/10.1680/geot.2008.58.8.623.

Hight, D.W. (2013). The 9th Victor de Mello lecture: reflections and speculations. *Soils and Rocks*, *47*(4), 1-29. http://doi.org/10.28927/SR.2024.008824.

ICMM. (2020). *Global industry standard on tailings management.* International Council of Mining and Metals, London.

ICOLD. (2005). *Bulletin 121 (2001): tailings dams risk of dangerous occurrences - lessons learnt from practical experiences; Bulletin 139 (2011): improving tailings dam safety - critical aspects of management, design, operation, and closure; Bulletin 153 (2013): committee on tailings dams - sustainable design and post-closure performance of tailings dams*. International Commission on Large Dams.

Jefferies, M.G. (1993). Nor-Sand: a simple critical state model for sand. *Geotechnique*, *43*(1), 91-103. http://doi.org/10.1680/geot.1993.43.1.91.

Jefferies, M., & Been, K. (2015). *Soil liquefaction: a critical state approach* (2nd ed.). New York: Taylor & Francis Group. http://doi.org/10.1201/b19114.

Jefferies, M., Morgenstern, N.R., Van Zyl, D.V., & Wates, J. (2019). *Report on NTSF embankment failure, Cadia Valley operations, for Ashurst Australia*. Independent Technical Review Board.

Jesus, M.H.D., Serafim, R., Silva, J.P., & Marinho, F.A. (2023). Unsaturated shear strength parameters for a compacted iron ore tailings. *E3S Web of Conferences*, *382*, 1-6.

Kulhawy, F.H., & Mayne, P.W. (1990). *Manual on estimating soil properties for foundation design*. Electric Power Research Institute.

Lade, P.V., & Yamamuro, J.A. (2011). Evaluation of static liquefaction potential of silty sand slopes. *Canadian Geotechnical Journal*, *48*(2), 247-264. http://doi.org/10.1139/T10-063.

Ledesma, O., Sfriso, A., & Manzanal, D. (2022). Procedure for assessing the liquefaction vulnerability of tailings dams. *Computers and Geotechnics*, *144*, 104632. http://doi.org/10.1016/j.compgeo.2022.104632.

Levandoski, W.M.K., Ferrazzo, S.T., Bruschi, G.J., Consoli, N.C., & Korf, E.P. (2023). Mechanical and microstructural properties of iron mining tailings stabilized with alkali-activated binder produced from agro-industrial wastes. *Scientific Reports*, *13*(1), 15754. http://doi.org/10.1038/s41598-023-42999-x.

Li, X.S., & Wang, Y. (1998). Linear representation of steady-state line for sand. *Journal of Geotechnical and Geoenvironmental Engineering*, *124*(12), 1215-1217. http://doi.org/10.1061/(ASCE)1090-0241(1998)124:12(1215).

Lucy, J.M. (2015). *Exploration and engineering of physical properties in high-quality Sr_2CrReO_6 epitaxial films* [Doctoral thesis]. Ohio State University's repository. Retrieved in December 28, 2024, from http://rave.ohiolink.edu/etdc/view?acc_num=osu1436888316

Lunne, T., Robertson, P.K., & Powel, J.J.M. (1997). *Cone Penetration Testing in Geotechnical Pratice* (2nd ed.). Taylor and Francis Group.

Mafessoli, M., Marques, S.F.V., Scheuermann Filho, H.C., & Consoli, N.C. (2023). Response of artificially cemented iron ore tailings for dry stacking disposal over a wide range of stresses. *Indian Geotechnical Journal*, *53*(4), 904-915. http://doi.org/10.1007/s40098-023-00711-w.

Medina, G.S., Farenzena, H.P., Bruschi, G.J., Rodrigues, B.D.A., Silva, J.P.D.S., Festugato, L., & Consoli, N.C. (2024). The behaviour of hydraulically disposed silty iron ore tailings under static and cyclic loading. *Geotechnical and Geological Engineering*, *42*(1), 1-19. http://doi.org/10.1007/s10706-024-02754-z.

Medina, G.S., Farenzena, H.P., Rodrigues, B.A., Silva, J.P., Festugato, L., & Consoli, N.C. (2023). Shear response of iron ore tailings under monotonic loadings. In *Proceedings of the 8th International Symposium on Deformation Characteristics of Geomaterials (IS-Porto 2023)*, Porto, Portugal.

Morgenstern, N.R. (August 28, 2018). Sixth victor de mello lecture: geotechnical risk, regulation, and public policy. In *Proceedings of the XIX Brazilian Conference on Soil Mechanics and Geotechnical Engineering – COBRAMSEG 2018*, Salvador, BA.

Morgenstern, N.R., Vick, S.G., Viotti, C.B., & Watts, B.D. (2016). *Fundão tailings dam review panel report on the immediate causes of the failure of the Fundão dam*. New York: Cleary Gottlieb Steen & Hamilton LLP.

Nadai, F. M., Marinho, F. A., & Silva, J. P. S. (2023). SWRC interpretation of iron ore tailings blends focusing on saturation assessment of dry stacking. *International Journal of Geotechnical Engineering*, 1-14. In press.

Nery, K.D. (2013). *Caracterização geotécnica e avaliação da compactação de um resíduo da produção de alumina (lama vermelha) desaguado por filtro prensa* [Master's dissertation]. Federal University of Minas Gerais (in Portuguese).

Nierwinski, H.P. (2019). *Characterization and geomechanical behavior of mining tailings* [Doctoral thesis]. Department of Civil Engineering, Federal University of Rio Grande do Sul.

Oliveira, S.C. (2022). *Influência do estado de tensão na obtenção dos parâmetros de estado crítico de rejeitos filtrados de minério de ferro* [Master's dissertation]. Federal University of Ouro Preto (in Portuguese).

Oliveira, F.W.A. (2025). *Avaliação da susceptibilidade à liquefação de uma pilha de rejeitos filtrados de terras* *raras* [Master's dissertation]. Federal University of Rio de Janeiro (in Portuguese).

Oliveira, S.C., Delgado, B.G., Paes, I.T., Viana da Fonseca, A.V., Pereira, E.L., & Paes, B.S.T. (2025). Influence of stress state on the expected behavior of filtered iron ore tailings for compacted stacking disposal. *Geotechnical Testing Journal*, *48*(2), 166-189. http://doi.org/10.1520/GTJ20230503.

Palmeira, E.M., Beirigo, E.A., & Gardoni, M.G. (2010). Tailings-nonwoven geotextile filter compatibility in mining applications. *Geotextiles and Geomembranes*, *28*(2), 136-148. http://doi.org/10.1016/j.geotexmem.2009.10.004.

Pereira, E.L. (2005). *Estudo do potencial de liquefação de rejeitos de minério de ferro sob carregamento estático* [Master's dissertation]. Federal University of Ouro Preto (in Portuguese).

Pereira, E., Gomes, R., & Ribeiro, L. (2006). Avaliação do potencial de liquefação estática de rejeitos de mineração. *Geotecnia*, (108), 151-173. http://doi.org/10.14195/2184-8394_108_9.

Pirete, W., & Gomes, R.C. (2013). Tailings liquefaction analysis using strength ratios and SPT/CPT results. *Soils and Rocks*, *36*(1), 37-53. http://doi.org/10.28927/SR.361037.

Pölzl, T., Telles, A.C.M., Fabre, J.S., Becker, L.B., & Barbosa, M.C. (2018). Análise de quebra de grãos em rejeito areno-siltoso submetido à ensaio de adensamento. In *Anais do XIX Congresso Brasileiro de Mecânica dos Solos e Engenharia Geotécnica*, Salvador, Brazil. UFOP.

Praca, L.P.L., Hoch, B.Z., Festugato, L., Schnaid, F., & Marques, S.F.V. (2019). Shear resistance of zinc mine tailings. In *Geotechnical Engineering in the XXI Century: Lessons Learned and Future Challenges: Proceedings of the XVI Pan-American Conference on Soil Mechanics and Geotechnical Engineering (XVI PCSMGE)* (pp. 339). IOS Press.

Quintelas, A.C.F., Becker, L.B., & Moura, M.V.S. (2020). The influence of relative density on the friction angle of iron ore tailings from the Fundão Dam. In *XIII International Symposium on Landslides*, Cartagena, Colombia. International Society for Soil Mechanics and Geotechnical Engineering.

Quirino, I.S., Fabre, J.S., Becker, L.B., & Barbosa, M.C. (2022). Análise da influência do teor de finos no ângulo de atrito de um rejeito de minério de ferro através de ensaios Ring Shear. In *Anais do XX Congresso Brasileiro de Mecânica dos Solos e Engenharia Geotécnica*, Campinas, Brazil.

Reid, D., & Fanni, R. (2020). A comparison of intact and reconstituted samples of a silt tailings. *Geotechnique*, *72*(2), 176-188. https://doi.org/10.1680/jgeot.20.P.020.

Reid, D., Chiaro, G., Fanni, R., & Fourie, A. (2022a). Arguments for increasing the use of hollow cylinder testing in the characterization of tailings. In *Proceedings of the Tailings and Mine Waste Conference*, Denver, USA.

Reid, D., Fanni, R., & Fourie, A. (2022b). Assessing the undrained strength cross-anisotropy of three tailings types. *Géotechnique Letters*, *12*(1), 1-24. http://doi.org/10.1680/jgele.21.00094.

Robertson, P.K., & Campanella, R.G. (1983). Interpretation of cone penetration tests: sands and clays. *Canadian Geotechnical Journal*, *20*(4), 719-745. https://doi.org/10.1139/t83-079.

Robertson, P.K. (2009). Interpretation of cone penetration tests: unified approach. *Canadian Geotechnical Journal*, *46*(11), 1337-1355. http://doi.org/10.1139/T09-065.

Robertson, P.K. (2016). Cone penetration test (CPT)-based soil behaviour type (SBT) classification system: an update. *Canadian Geotechnical Journal*, *53*(12), 1910-1927. http://doi.org/10.1139/cgj-2016-0044.

Robertson, P.K., Melo, L., Williams, D.J., & Wilson, G.W. (2019). *Report of the expert panel on the technical causes of the failure of Feijão Dam I.* Skadden, Arps, Slate, Meagher & Flom LLP.

Rógenes, E., Paes, I.T., Delgado, B.G., Bittar, R.J., Gomes, A.S., Cirone, A., Fávero Neto, A.H., & Rasmussen, L.L. (2025). Assessing static liquefaction triggers in tailings dams using the critical state constitutive models CASM and NorSand. *International Journal for Numerical and Analytical Methods in Geomechanics*, *49*(4), 1092-1112. http://doi.org/10.1002/nag.3914.

Saar, R.C., Santos, L.P.B., Almeida, M.S.S., & Delgado, B.G. (September 24-27, 2024). Avaliação da ocorrência de drenagem parcial nos ensaios de CPTu em rejeito de minério de ferro [Evaluation of partial drainage occurrence on iron ore tailings during CPTu tests]. In *Proceedings of the XXI Brazilian Congress of Soil Mechanics and Geotechnical Engineering*, Balneário Camboriú, Brazil. (in Portuguese).

Santos Junior, M.P., Gomes, R.C., Ribeiro, S.S., & Delgado, B.G. (2022). Evaluation of flow liquefaction susceptibility of a sandy-silt tailings using the CPTu. In G. Gottardi & L. Tonni (Eds.), *Cone penetration testing 2022* (pp. 913-919). London; CRC Press. http://doi.org/10.1201/9781003308829-119

Santos, C.P., Bruschi, G.J., Mattos, J.R.G., & Consoli, N.C. (2022). Stabilization of gold mining tailings with alkali-activated carbide lime and sugarcane bagasse ash. *Transportation Geotechnics*, *32*, 100704. http://doi.org/10.1016/j.trgeo.2021.100704.

Santos, R.A., Delgado, B.G., Rissoli, A.L.C., Silva, J.P.S., & Dal Toé Casagrande, M. (2023). Influence of initial compaction and confining pressure on the hydraulic conductivity of compacted iron ore tailings. In *Proceedings of the 8th International Symposium on Deformation Characteristics of Geomaterials (IS-Porto 2023)*, Porto, Portugal.

Sasitharan, S., Robertson, P.K., Sego, D.C., & Morgenstern, N.R. (1993). Collapse behavior of sand. *Canadian Geotechnical Journal*, *30*(4), 569-577. http://doi.org/10.1139/t93-049.

Schnaid, F. (2019). On the geomechanics and geocharacterization of tailings. In *Proceedings of the 6th International Conference on Geotechnical and Geophysical Site Characterization (ISC2020)*. ISSMGE. http://doi.org/10.53243/ISC2020-501

Schnaid, F., Bedin, J., Viana da Fonseca, A.J.P., & Costa Filho, L.M. (2013). Stiffness and strength governing the static liquefaction of tailings. *Journal of Geotechnical and Geoenvironmental Engineering*, *139*(12), 2136-2144. http://doi.org/10.1061/(ASCE)GT.1943-5606.0000924.

Schnaid, F., Martins, I.S.M., Delgado, B.G., & Odebrecht, E. (2021). Velocidade de carregamento na estimativa de parâmetros geotécnicos. *Geotecnia*, *12*(152), 405-434. http://doi.org/10.14195/2184-8394_152_12.

Schnaid, F., Nierwinski, H.P., Bedin, J., & Odebrecht, E. (2014). On the characterization and classification of bauxite tailings. *Soils and Rocks*, *37*(2), 277-284. http://doi.org/10.28927/SR.373277.

Schofield, A.N., & Wroth, C.P. (1968). *Critical state soil mechanics.* London: McGraw Hill.

Servi, S., Lotero, A., Silva, J.P.S., Bastos, C., & Consoli, N.C. (2022). Mechanical response of filtered and compacted iron ore tailings with different cementing agents: focus on tailings-binder mixtures disposal by stacking. *Construction & Building Materials*, *349*, 128695. http://doi.org/10.1016/j.conbuildmat.2022.128770.

Shibuya, S., Highi, D., & Jardine, R.J. (2003). Four-dimensional local boundary surfaces of an isotropically consolidated loose sand. *Jiban Kogakkai Ronbun Hokokushu*, *43*(2), 89-103. http://doi.org/10.3208/sandf.43.2_89.

Shuttle, D., Basile, S., Marinelli, F., & Jefferies, M. (2021). Validation of computational liquefaction for tailings: Tar Island slump. *Geotechnical Research*, *9*(1), 32-55. http://doi.org/10.1680/jgere.21.00007.

Silva, V.L., Gardoni, M.G.A., & Pimentel, K.C. (2021). Numerical modelling of geotextile tubes filled with gold mine tailings. *Geosynthetics International*, *28*(6), 574-583. http://doi.org/10.1680/jgein.21.00017.

Silva, J.P.D.S., Carvalho, J.V.D.A., Wagner, A.C., Cacciari, P.P., & Consoli, N.C. (2023). On the mechanics of filtered compacted consolidated and overconsolidated iron ore tailings at high pressures. *Canadian Geotechnical Journal*, *61*(3), 575-581. http://doi.org/10.1139/cgj-2023-0056.

Silva, J.P.S., Rissoli, A.L.C., Cacciari, P.P., Fonseca, A.J.P.V., Scheuermann Filho, H.C., Wagner, A.C., Carvalho, J.V.A., Festugato, L., & Consoli, N.C. (2024). Triaxial testing response of compacted iron ore tailings considering a broad spectrum of confining pressures. *Soil and Foundation*, *64*(2), 101438. http://doi.org/10.1016/j.sandf.2024.101438.

Skopek, P., Morgenstern, N.R., Robertson, P.K., & Sego, D.C. (1994). Collapse of dry sand. *Canadian Geotechnical Journal*, *31*(6), 1003-1008. http://doi.org/10.1139/t94-115.

Soares, M., & Viana da Fonseca, A. (2016). Factors affecting steady state locus in triaxial tests. *Geotechnical Testing Journal*, *39*(6), 1056-1078. http://doi.org/10.1520/GTJ20150228.

Souza, A.J.P. (2023). *Instability of the Fundão sand tailings under lateral extrusion stress path with different drainage condition in triaxial and hollow cylinder tests* [Master's dissertation]. Federal University of Rio de Janeiro.

Souza, A.J., Telles, A.C., Reid, D., Fourie, A., & Almeida, M.S.S. (2024). Instability of sand under a lateral extrusion stress path with different drainage conditions. *Soil and Foundation*, *64*(6), 101529. http://doi.org/10.1016/j.sandf.2024.101529.

Telles, A.C.M. (2017). *Análise do comportamento de um rejeito de minério de ferro no estado de regime permanente* [Master's dissertation]. Federal University of Rio de Janeiro (in Portuguese).

Telles, A.C.M., Becker, L.B., & Silva, C.G.C. (2019). Influência do teor de finos no comportamento mecânico de um rejeito de minério de ferro. In *Anais do IX Congresso Brasileiro de Geotecnia Ambiental (REGEO 2019)*, São Carlos, SP.

Tinoco, C.P., & Marinho, F.A. (November 17-20, 2019). Shear strength characteristics of a bauxite tailing. In *Geotechnical Engineering in the XXI Century: Lessons Learned and Future Challenges: Proceedings of the XVI Pan-American Conference on Soil Mechanics and Geotechnical Engineering (XVI PCSMGE)* (p. 319), Cancun, Mexico. IOS Press.

Torres-Cruz, L.A., & Santamarina, J.C. (2020). The critical state line of nonplastic tailings. *Canadian Geotechnical Journal*, *57*(10). http://dx.doi.org/10.1139/cgj-2019-0019.

Treadwell, D.D. (1976). *The influence of gravity, prestress, compressibility, and layering on soil resistance to static penetration* [Doctoral thesis]. University of California at Berkeley.

Uthayakumar, M., & Vaid, Y.P. (1998). Static liquefaction of sands under multiaxial loading. *Canadian Geotechnical Journal*, *35*(2), 273-283. http://doi.org/10.1139/t98-007.

Velten, R.Z., Consoli, N.C., Filho, H.C.S., Wagner, A.C., Schnaid, F., & Costa, J.P.R. (2024). Influence of grading and fabric arising from the initial compaction on the geomechanical characterisation of compacted copper tailings. *Geotechnique*, *74*(5), 461-472. http://doi.org/10.1680/jgeot.22.00087.

Viana da Fonseca, A., Cordeiro, D., & Molina-Gómez, F. (2021). Recommended procedures to assess critical state locus from triaxial tests in cohesionless remoulded samples. *Geotechnics*, *1*(1), 95-127. http://doi.org/10.3390/geotechnics1010006.

Viana da Fonseca, A., Cordeiro, D., Molina-Gómez, F., Besenzon, D., Fonseca, A., & Ferreira, C. (2022). The mechanics of iron tailings from laboratory tests on reconstituted samples collected in post-mortem Dam I in Brumadinho. *Soils and Rocks*, *45*(2), 1-20. http://doi.org/10.28927/SR.2022.001122.

Vilar, O.M. (2006). A simplified procedure to estimate the shear strength envelope of unsaturated soil. *Canadian Geotechnical Journal*, *43*(10). https://doi.org/10.1139/t06-055.

Wagner, A.C., Sousa Silva, J.P., Carvalho, J.V.A., Rissoli, A.L.C., Cacciari, P.P., Chaves, H.M., Scheuermann Filho, H.C., & Consoli, N.C. (2023). Mechanical behavior of iron ore tailings under standard compression and extension triaxial stress paths. *Journal of Rock Mechanics and Geotechnical Engineering*, *15*(7), 1883-1894. http://doi.org/10.1016/j.jrmge.2022.11.013.

Wagner, A.C., Carvalho, J.V.A., Scheuermann Filho, H.C., & Consoli, N.C. (2024a). Influence of grading in compacted tailings behaviour: towards resilient design. *Geotechnique*, 1-14. In press. http://doi.org/10.1680/jgeot.23.00475.

Wagner, A.C., Carvalho, J.V.D.A., Sousa Silva, J.P., Scheuermann Filho, H.C., & Consoli, N.C. (2024b). Dry stacking of iron ore tailings: Possible particle breakage during compaction. *Proceedings of the Institution of Civil Engineers - Geotechnical Engineering*, *177*(6), 779-787. http://doi.org/10.1680/jgeen.22.00216.

Wang, Y., Vo, T., & Russell, A.R. (2023). Modelling unsaturated silty tailings and the conditions required for static liquefaction. *Geotechnique*, *74*(12), 1377-1389. http://dx.doi.org/10.1680/jgeot.22.00074.

Watson, A.H., Corser, P.G., Garces Pardo, E.E., Lopez Christian, T.E., & Vandekeybus, J. (September, 2010). A comparison of alternative tailings disposal methods: the promises and realities. In *Mine Waste 2010: Proceedings of the First International Seminar on the Reduction of Risk in the Management of Tailings and Mine Waste* (pp. 499-514). Australian Centre for Geomechanics. http://doi.org/10.36487/ACG_rep/1008_41_Watson.

Zabolotnii, E. (2020). *Three-dimensional slope stability effects in the failure at the Mount Polley Tailings Storage Facility* [Doctoral thesis]. University of Alberta, Edmonton, Alta, Canada.